

Numerical Modeling of Tsunami Effects at Marine Oil Terminals in San Francisco Bay

Jose Borrero¹, Lori Dengler², Burak Uslu¹, Costas Synolakis¹

Report Prepared for:
Marine Facilities Division of The California State Lands Commission,

June 8, 2006

¹ Department of Civil Engineering, University of Southern California, Los Angeles 90089

² Geology Department, Humboldt State University, Arcata California 95521

Table of Contents

Executive Summary.....	1
1. Introduction.....	3
2. San Francisco Bay tsunami history.....	5
2.1 Historical teletsunamis.....	5
2.1.1 1960 Chilean tsunami in San Francisco Bay.....	6
2.1.2 1964 Alaskan tsunami in San Francisco Bay.....	7
2.2 Historical local tsunamis.....	9
2.2.1 1868 Hayward fault earthquake.....	10
2.2.2 1898 Mare Island earthquake.....	11
2.2.3 1906 San Francisco earthquake.....	11
3. Prior research on San Francisco Bay tsunami hazards.....	12
4. Numerical method and model.....	14
4.1 Numerical grids.....	15
5. Tsunami sources.....	17
5.1 Subduction zones.....	17
5.1.1 Cascadia subduction zone.....	20
5.1.2 Alaska and the Aleutian Islands.....	20
5.1.3 Kuril Islands.....	21
5.1.4 Japan.....	21
5.1.5 South America.....	22
5.2 Near-field sources.....	22
5.2.1 San Gregorio fault.....	23
5.2.2 Hayward – Rogers Creek fault step-over.....	23
5.2.3 Farallon Islands landslide.....	24
5.2.4 Other sources.....	24
6. Results and discussion.....	25
6.1 Comparison to historical data.....	27
6.2 Effect of source region.....	29
6.3 A worst-case scenario?.....	31
6.4 Recommendations for terminal sites.....	34
Acknowledgements.....	35
References.....	36
Appendices	
Appendix 1 Model results	
Table A1-1: Name and locations of Marine Oil Terminals.....	1
Alaska 1964.....	3
Aleutians I.....	8
Aleutians II.....	13
Aleutians III.....	18
Kuril I.....	23
Kuril II.....	28

Kuril III.....	33
Kuril IV.....	38
Japan I.....	43
Japan II.....	48
Chile 1960.....	53
Chile 1960W.....	59
N Chile.....	65
Cascadia I.....	71
Cascadia II.....	76
Cascadia III.....	81
Cascadia SN.....	86
Cascadia SW.....	91
Cascadia SP2.....	96
Hayward-Rodgers Creek.....	101
San Gregorio.....	106
Farallons.....	111

Appendix 2 Maximum water heights and current velocities

Table A2-1: Name and locations of Marine Oil Terminals.....	1
Table A2-2: Alaska 1964.....	2
Table A2-3: Aleutians I.....	2
Table A2-4: Aleutians II.....	3
Table A2-5: Aleutians III.....	3
Table A2-6: Kuril I.....	4
Table A2-7: Kuril II.....	4
Table A2-8: Kuril III.....	5
Table A2-9: Kuril IV.....	5
Table A2-10: Japan I.....	6
Table A2-11: Japan II.....	6
Table A2-12: Chile 1960.....	7
Table A2-13: Chile 1960W.....	7
Table A2-14: N Chile.....	8
Table A2-15: Cascadia I.....	8
Table A2-16: Cascadia II.....	9
Table A2-17: Cascadia III.....	9
Table A2-18: Cascadia SN.....	10
Table A2-19: Cascadia SW.....	10
Table A2-20: Cascadia SP2.....	11
Table A2-21: Hayward-Rodgers Creek.....	11
Table A2-22: San Gregorio.....	12
Table A2-23: Farallons.....	12

Appendix 3 Historic San Francisco Bay tsunami events

Appendix 4 Historic California tsunami events

Appendix 5 The 1964 tsunami in San Francisco Bay

Appendix 6 Tide gauge records for May 22, 1960 and March 28, 1964

Tables

Table 1	Source regions of historic San Francisco Bay tsunamis.....	5
Table 2	1960 recorded wave heights.....	6
Table 3	Local and regional tsunamis.....	10
Table 4	Marine oil terminal (MOT) locations.....	16
Table 5	Scenario source parameter summary.....	19
Table 6	Peak water height summary.....	25
Table 7	Composite sources referenced in Figure 19.....	30
Table 8	Maximum computed values of water rise and fall.....	33
Table 9	Maximum computed values of current velocity.....	33
Table 10	Peak water heights and current velocity recommendations.....	34

Figures

Figure 1	San Francisco Bay Area.....	3
Figure 2	Bathymetry and topography of San Francisco Bay.....	4
Figure 3	Bay Area historic tsunami locations.....	5
Figure 4	1960 tsunami tide gauge records.....	7
Figure 5	1964 tsunami tide gauge records.....	8
Figure 6	Teletsunami attenuation model.....	9
Figure 7	Right step-over.....	11
Figure 8	Ritter and Dupre Bay Area inundation map.....	12
Figure 9	Frequency of occurrence of peak tsunami height.....	13
Figure 10	Marine Oil Terminal locations.....	15
Figure 11	Coverage areas for numerical grid regions.....	16
Figure 12	North Pacific far-field tsunami source regions.....	17
Figure 13	Pacific Rim subduction zone fault segments.....	18
Figure 14	Potential local tsunami sources.....	22
Figure 15	Comparison of scenario water heights.....	26
Figure 16	1960 tsunami comparison of modeled and actual water levels.....	27
Figure 17	1964 tsunami comparison of modeled and actual water levels.....	28
Figure 18	Computed wave height at Bay entrance for unit slip sources.....	29
Figure 19	Scenario maximum positive and negative wave heights.....	31
Figure 20	Comparison of 1964 and worst case tsunami.....	32

Executive Summary

Tsunami-induced wave heights and current velocities are investigated at Marine Oil Terminal (MOT) sites in San Francisco Bay. Marine Oil Terminals are locations where tank vessels (tankers) load and offload petroleum products to or from facilities on land for refining or distribution. We conducted a deterministic study to identify the most severe events that could reasonably impact the Marine Oil Terminal sites.

During historic times, 51 credible tsunamis have been recorded or observed in the San Francisco Bay region. Of these, only 5 produced runup that likely exceeded 0.5 m (1.6 ft) within the Bay. The best-documented tsunami events are the 1946, 1960 and 1964 tsunamis generated by distant earthquakes in Aleutian Islands, Southern Chile and Prince William Sound, Alaska respectively. In addition, three local tsunamis in the 19th century may also have generated waves in excess of 0.5 m (1.6 ft), however none were recorded on tide gages and the height is estimated from eyewitness accounts only.

We selected a suite of sources with the potential to impact San Francisco Bay based on historic events, Pacific basin tectonics, and regional seismicity to initialize our numerical simulations. Both near- and far-field sources were considered; far-field sources included large magnitude subduction zone earthquakes around the Pacific Rim while near-field sources are faults, step-over structures and potential landslide sources just offshore of the San Francisco Bay entrance and within the Bay itself.

We used the numerical model MOST (Titov and Gonzales, 1997; Titov and Synolakis, 1998) to simulate tsunami generation, propagation and runup. MOST uses an elastic deformation model to initialize the computation then solves the 2 dimensional shallow water wave equations to propagate the disturbance across an ocean basin. The robustness of the MOST model for San Francisco Bay is demonstrated through replication of recorded marigrams for the 1960 and 1964 tsunamis.

Twenty-three scenarios were modeled, ranging from a landslide in the Farallon Islands to a magnitude 6.6 earthquake in San Pablo Bay (the northern arm of San Francisco Bay) and magnitude 9+ earthquakes on subduction zones around the Pacific Rim. The model results allow an estimation of the maximum credible tsunami water heights at the MOT sites and a sensitivity study of sources likely to produce the greatest impacts.

Results suggest that large ruptures along the Alaska Peninsula and eastern segments of the Alaska-Aleutian subduction zone present a much greater hazard than any other source region either locally or in the Pacific. The greatest hazard is for terminals in the Richmond area caused by very large ($M_w > 9$) earthquakes on these segments of the Alaska-Aleutian subduction zone. Direct output from our modeling suggests these earthquakes could produce positive waves of over 5 m (16.4 ft) at the entrance to San Francisco Bay and 1.6 m (4.88 ft) at MOTs in Richmond, CA. A maximum drawdown (negative wave) of -3.74 m (-12.27 ft) and -1.6 m (-5.88 ft) would also be expected at these sites. Associated maximum current speeds at select locations would be on the order of 2 – 5 m/s (3.9 – 9.7 knots).

The results also suggest that the Cascadia subduction zone along the Pacific Northwest coast of Northern California to Southern British Columbia presents only a moderate tsunami hazard for locations within San Francisco Bay. The largest local event is produced by the step-over rupture of the Hayward fault to the Rogers Creek fault beneath San Pablo Bay, but it is significantly smaller than tsunamis generated by large events on the Alaska-Aleutian subduction zone. A large landslide on the Farallon Islands offshore of San Francisco Bay only produces peak water heights within the Bay of about 20 cm (.7 ft).

Based on our modeling results and a conservative factor of safety, we estimate maximum credible tsunami amplitudes at MOT locations in the Richmond area of 2.4 m (7.9 ft) and a current velocity of 2.7 m/sec (5.2 knots), in the western Carquinez Straits of 0.8 m (5.9 ft) and a current velocity of 0.6 m/sec (1.2 knots) and in the Portrero District of San Francisco of 1.8 m and 1.5 m/sec (2.9 knots). All of these values are significantly below the estimates of Garcia and Houston (1975).

1. INTRODUCTION

San Francisco Bay (Figure 1) is located on the west coast of North America. It is a mostly enclosed body of water with a narrow opening (the Golden Gate) to the North Pacific Ocean at approximately 37.8° N and 122.5° W (237.5° E). The Bay is fed mainly by river flows from the Sacramento, San Joaquin and Napa Rivers as well as many other minor streams. San Francisco Bay and its northern arm, San Pablo Bay, cover some 4100 square kilometers. The Bay is located within the San Andreas transform fault system, part of the boundary between the Pacific and North American tectonic plates. The majority of the slip on this plate boundary is accommodated by the San Andreas Fault, however part of the relative plate motions are taken up by several other smaller faults. Three earthquakes of likely magnitude 7 or larger and numerous smaller events have occurred in the Bay region in historic times.

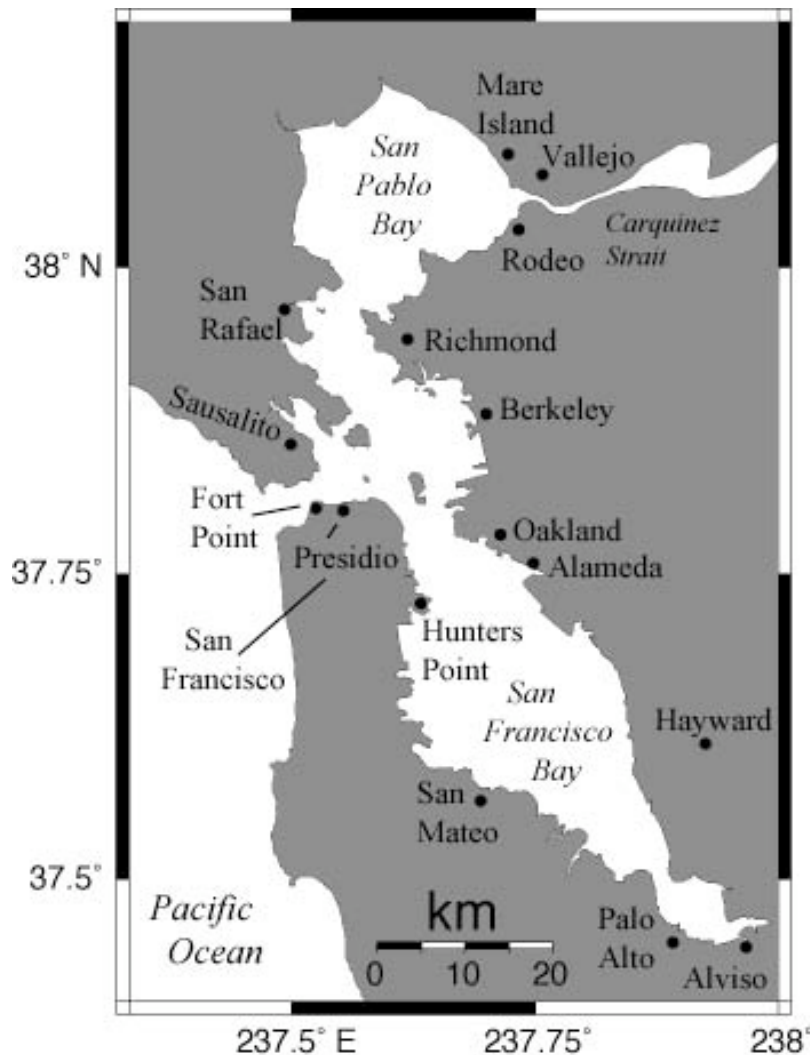


Figure 1 – San Francisco Bay area.

The San Francisco Bay area is home to approximately 6.8 million people, most of who live on coastal lands (USGS, 2002). San Francisco Bay is heavily industrialized and includes major port facilities in Oakland and San Francisco and fifteen marine oil terminals (MOTs) where petroleum products are transferred between ships and refineries on shore (California Building Code, 2001). The marine oil terminals are generally located on the eastern shore of the Bay near the cities of Oakland, Richmond and Vallejo. The list of terminals is given in Table 4 and their locations shown on Figure 3 and 10.

The bathymetry of San Francisco Bay is shown in Figure 2. Much of San Pablo Bay and the southern section of San Francisco Bay are quite shallow with depths generally less than 20 m (66 ft). In the central section of the Bay and near the Golden Gate, there is more bathymetric relief. The deepest part of the Bay is beneath the Golden Gate with depths of over 100 m (328 ft). The shallow bathymetry is a factor in the tsunami wave dynamics within the bay, as it attenuates tsunami waves that propagate through the bay.

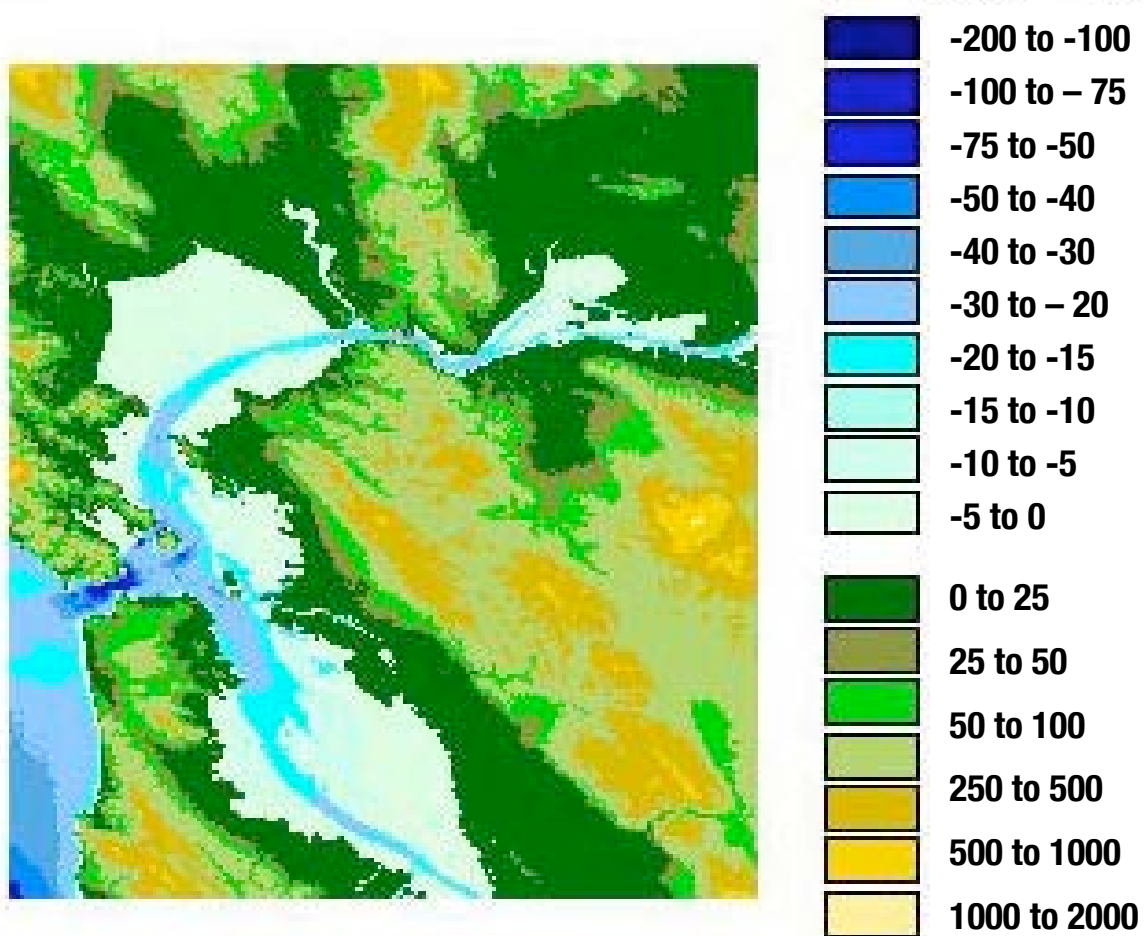


Figure 2 – Bathymetry and topography of San Francisco Bay. Colors represent the depth/elevation (in meters) for the intervals shown on the right.

2. SAN FRANCISCO BAY TSUNAMI HISTORY

During historic times, 51 credible tsunamis have been recorded or observed within the San Francisco Bay area (Table 1, Figure 3, also see Appendix 3).

Table 1 - Source Regions of Historic San Francisco Bay Tsunamis

Region	Number
SF Bay	6
Other California	2
Japan	9
Kurils and Kamchatka	7
Alaska and Aleutians	9
Hawaii	2
South America	10
SW Pacific	3
Central America	1
Unknown teletsunami	2
TOTAL	51

From Lander et al., 1993 and the NGDC

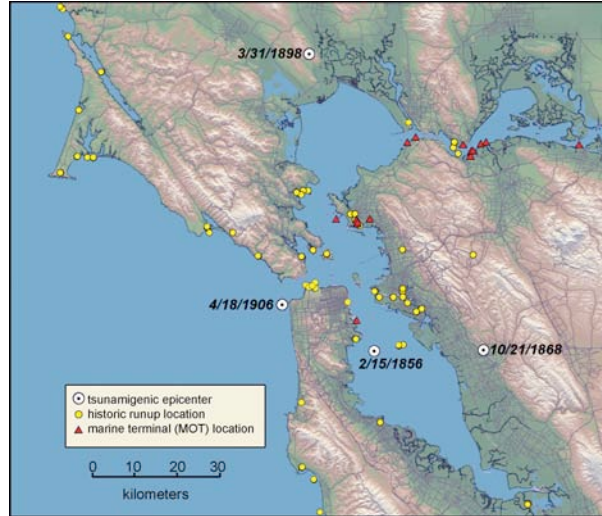


Figure 3 – Historic tsunami runup sites (yellow dots), tsunamigenic epicenters (white dots) and Marine Oil Terminal (MOT) locations.

Only 5 historic tsunamis produced runup that likely exceed 0.5 m (1.6 ft) within the San Francisco Bay (Appendix 3). The best-documented tsunami events are the 1946, 1960 and 1964 teletsunamis generated by earthquakes in the Aleutian Islands, Southern Chile and Prince William Sound, Alaska respectively. In addition, three local tsunamis in the nineteenth century may also have generated waves in excess of 0.5 m (1.6 ft), however none were recorded on tide gages and the height is estimated from eyewitness accounts only.

San Francisco Bay has had a tide gauge in place since 1854. The gauge has operated at three different sites, and the precise location has not always been clear. It was first installed at Fort Point for the years between 1854 and 1877, and then moved to Sausalito from 1877 through 1897. In 1897 the gauge was moved to its present location at the Presidio (Bromirski et al., 2000). Although the gauge has been in continuous operation since then, some of the records have been lost or events were not recorded due to instrumental problems or severe weather conditions. Other stations have operated on an interim basis including Hunters Point, Alameda, Oakland and Mare Island (see Figure 1). An array of temporary instruments was deployed after the 1960 Chilean earthquake including 33 instruments in the Bay and inland along the San Joaquin and Sacramento Rivers (Magoon, 1962).

2.1 HISTORICAL TELETsunamiS

Forty-three of the 51 historic tsunamis recorded or observed in San Francisco Bay come from teletsunami sources of at least 4 hours travel time (Table 1). The most common

source area is the northwestern Pacific (Japan and the Kamchatka-Kuril Trench), followed by South America and Alaska/Aleutian Islands as shown in Table 1. Of these, only two events caused damage in San Francisco Bay, tsunamis generated by the 1960 M_w 9.5 Chile earthquake and the 1964 M_w 9.2 Alaska earthquake.

2.1.1 The 1960 Chilean tsunami in San Francisco Bay

On May 22, 1960 a large earthquake in southern Chile generated a tsunami with runup in the immediate source area reaching at least 25 m (82 ft) (Instituto Hidrografico de la Armada, 1982) and causing over 1200 deaths. The tsunami crossed the Pacific and caused damage throughout the Pacific basin and additional casualties in Hawaii and Japan. The wave caused over \$1 million in damage in Los Angeles and Long Beach harbors as well as a 3.9 m (13 ft) rise in sea level and associated runup in Crescent City (NGDC).

The tsunami waves from this event began arriving in San Francisco Bay on the morning of May 23rd, approximately 15 hours after the earthquake. The tsunami was recorded on the tide gauges at the Presidio and Alameda as well as on a 33-gauge array of water level recorders present in San Francisco Bay during the tsunami event (Magoon, 1962). The waves were observed on 6 of the 33 gauges and the maximum recorded wave heights are shown in Table 2.

Location	Max. wave height (m)
Presidio	0.88
Hunters Point	0.12
Alameda	0.58
Oakland	0.37
Carquinez Strait	0.03
Benicia	0.06

Table 2 - 1960 recorded wave heights from Magoon (1962)

Figure 4 shows the tide gauge recordings from the Presidio and Alameda. The tidal signal has been removed from these records; the original unfiltered records are shown in Appendix 6. The plots illustrate a feature of many recorded tsunamis within the bay. The initial cycle is relatively long period (72 minutes) followed by shorter period oscillations (about 30 minutes) and lasts more than 12 hours. The fundamental free period for oscillations in the bay is 114 min, the second harmonic is about 57 minutes and the third harmonic is 38 minutes (Wilson and Torum, 1967). Wilson and Torum speculate that the long duration short period oscillations are the result of near-resonance with the third harmonic that develops as a result of entrance constriction at the Golden Gate. The marigrams also illustrate the attenuation of wave energy as the waves transit the bay. The amplitude of the Alameda signal is about half the strength of the Presidio site. It should be emphasized that the largest waves recorded on the time series occurred some 4 to 8 hours after the first wave arrival. The only reported damage in the bay was a

catamaran yacht torn from its moorings in a lagoon north of the Golden Gate (Magoon, 1962). The San Francisco Ferry Service was disrupted by a current “running like the Mississippi River” (Lander et al., 1993).

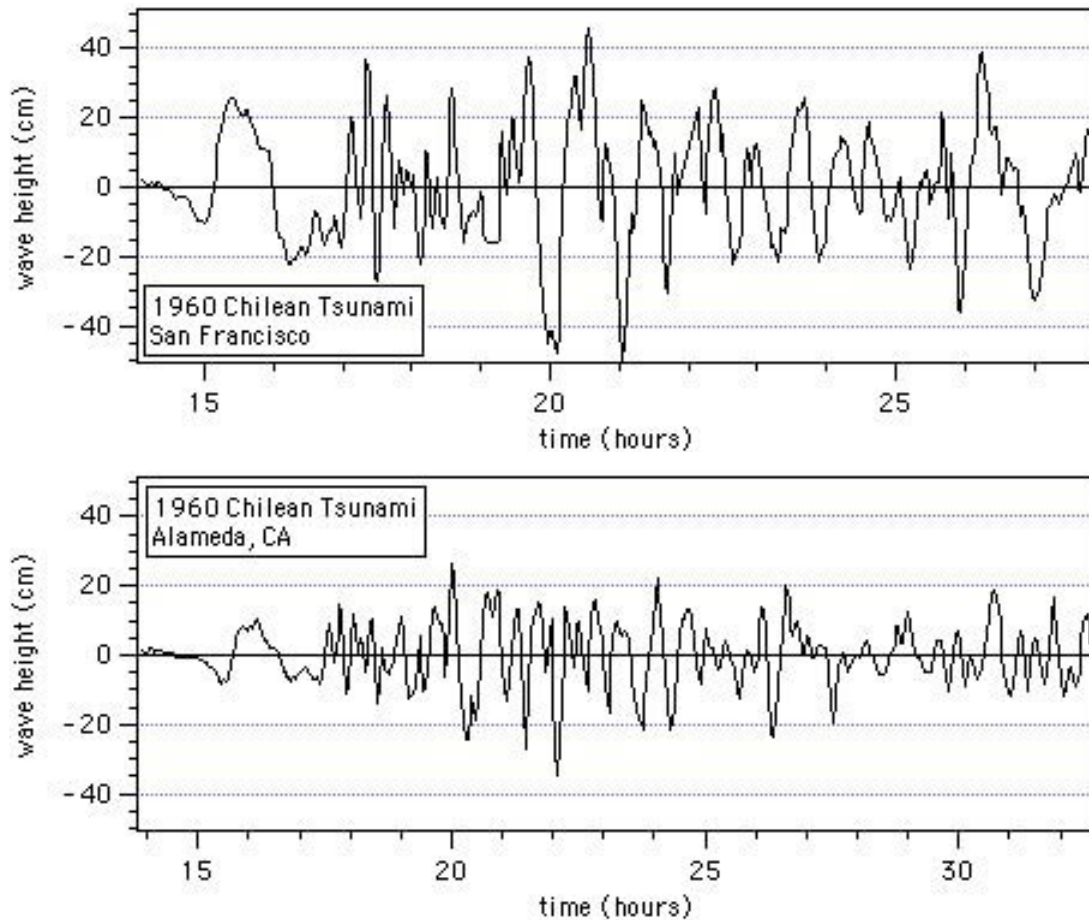


Figure 4 – Filtered tide gauge records (tide signal removed) from the first twelve hours of the 1960 Chilean tsunami at The Presidio (upper panel) and Alameda (lower panel). The time is in hours after the earthquake.

2.1.2 The 1964 Alaskan tsunami in San Francisco Bay

On March 28, 1964 a magnitude (M_w) 9.2 earthquake struck the Prince William Sound area of Alaska. The earthquake generated a tsunami that caused tsunami runup in excess of 60 m (197 ft) in Alaska. The tsunami waves strongly affected the California coast and caused significant damage to Crescent City as well as damage and flooding in San Francisco Bay. There were 12 fatalities in California, including 11 in Crescent City. Lander et al. (1993) report wave heights up to 2.1 m (7 ft) affecting areas inside San Francisco Bay. The strongest effects were observed in the northeastern parts of the bay, particularly in Sausalito and other Marin County locations on the Bay. Strong surges and high water were also observed in Berkeley, Richmond and Oakland. Damage included boats being torn from moorings, damaged docks and piers as well as floating docks, which came loose and were carried away from their original locations. Damage estimates

ranged up to \$17 million statewide including \$1 million in the San Francisco Bay area (Lander et al., 1993).

The tsunami was noted at 27 sites within the bay (Appendix 5) and caused damage to boats and floating structures (Magoon, 1966). There were numerous reports of strong currents within the bay. The largest amplitude waves were at the Presidio where the second oscillation had a 2.3 m (7.5 ft) peak to trough amplitude. Had the largest waves coincided with high tide, the absolute water level could have reached 3.8 m (12.5 ft) above sea level at the Presidio. Tide gauge records from the 1964 event at the Presidio and Alameda are shown in Figure 5. Spectral analysis by Wilson and Torum (1967) of the 1964 Presidio marigram identified 2 dominant periods in addition to the tidal forcing, a 100-minute period and a 38.5-minute period. They attribute the shorter period to resonance with the third harmonic of the bay oscillation and conclude that the geometry of the bay entrance will excite this period for any large tsunami entering through the Golden Gate.

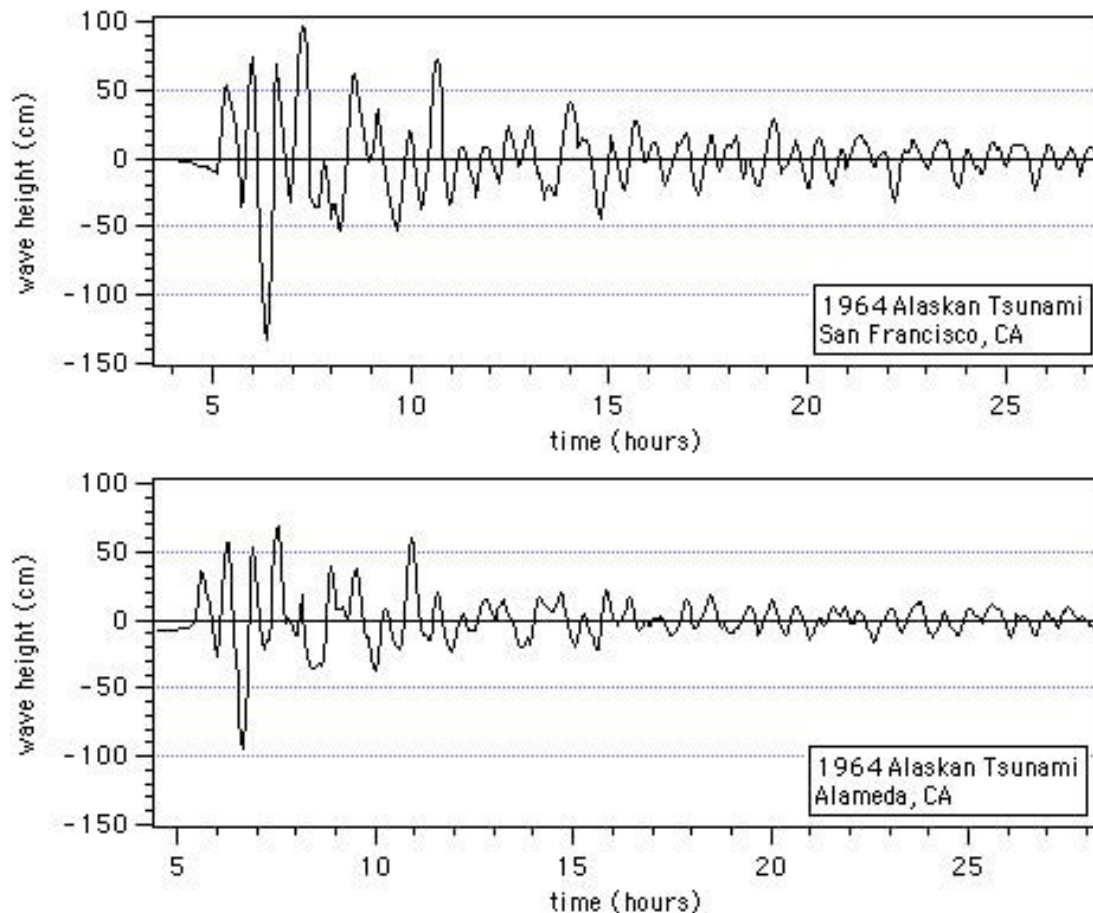


Figure 5 – Filtered tidal gauge records (tide signal removed) from the 1964 tsunami recorded at The Presidio (upper panel), and Alameda (lower panel). The time coordinate is in hours after the earthquake.

Magoon (1966) compiled runup data from both the 1960 and 1964 tsunamis within the bay and developed an empirical attenuation model (Figure 6). According to his data, the tsunami wave height was reduced by 50% between the Presidio, just inside the Golden Gate, and at Hunter's Point on the San Francisco Peninsula and Richmond or Oakland on the eastern shore of the Bay. The wave height was further reduced to 10% of its original height by the time it reached the northwestern shore of San Pablo Bay and the southern end of San Francisco Bay.

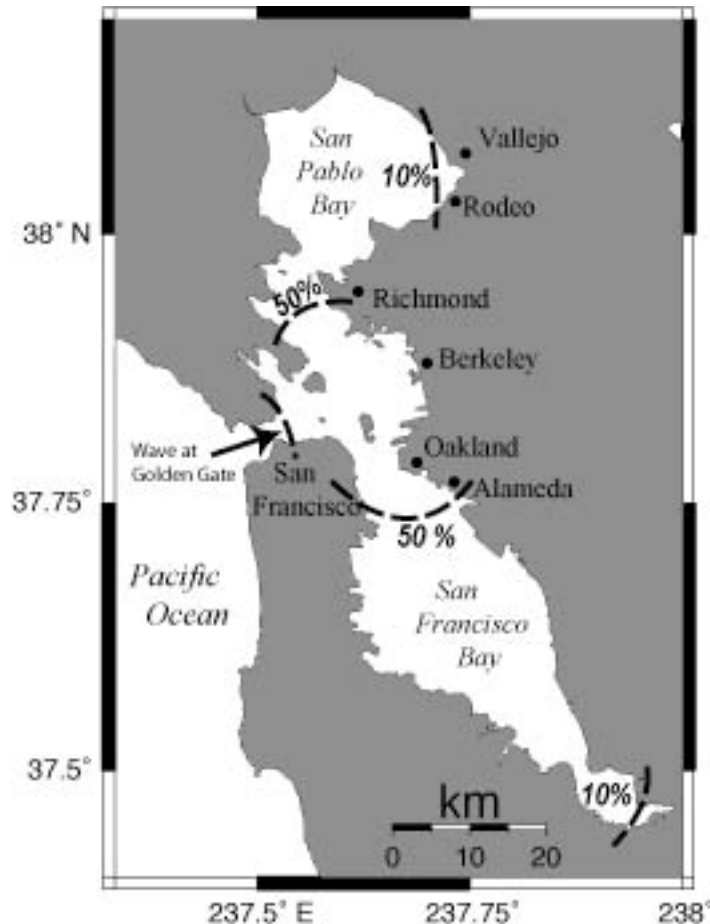


Figure 6 – Teletsunami attenuation model for San Francisco Bay based on observations from the 1960 (Chile) and 1964 (Alaska) tsunamis. (Magoon, 1966).

2.2 HISTORICAL LOCAL TSUNAMIS

Six credible local-source tsunamis and several possible tsunamis are documented for the San Francisco area. Two additional tsunamis were recorded from other source regions in northern California (Table 3). Of the 6 credible local source events, 4 were probably caused by earthquakes and 2 by earthquake-triggered landslides. One event in 1887 was associated with no known earthquake and, if real, may represent slumping within the bay. Perhaps the most notable aspect of historic local-source tsunamis is that they all occurred in the 19th and early 20th century. Topozada (personal communication) suggests that the

high frequency of local events in the late 1800's reflects the overall activity of the San Andreas system prior to the 1906 San Francisco earthquake.

Table 3 - Local and regional San Francisco tsunamis

Year Month/ day	Source area	V*	C**	Location of Effects	Runup (m)	Comments
1851 11/13	N. California San Francisco	1	E	San Francisco Bay	Observed	Unusual water movement felt on ship. Possible seiche.
1852 11/25	N. California San Francisco	1	E	San Francisco	Observed	Lake Merced drained.
1854 10/22	N. California San Francisco	2-3	E	San Francisco	Observed	Vessels swayed. Water rose 0.6 m with high waves in calm weather near Angel Island.
1856 2/15	N. California San Francisco	3	L	San Francisco	0.6	Water rose and stayed high for 5 minutes. Followed M 5.9 quake.
1868 10/21	N. California Hayward fault 7.0 earthquake	1 1 3	L	Government Isl. Sacramento San Francisco	Observed Observed 4.5	Registered on tide gauge. 0.61 m wave observed. 6.0 m surge at Cliff House.
1869 2/10	N. California San Francisco	1	M	San Francisco	Observed	Earthquake recorded on tide gage?
1869 6/1	N. California	3	E?	San Francisco	Observed	Earthquake waves Recorded
1887 7/8	N. California	2	L?	Sausalito	Observed	Distinct waves. No source known.
1898 3/31 ³	N. California 6.7 EQ Rogers Cr. fault	3	E	San Francisco Bay	0.6	Earthquake on the Rogers Creek fault. Tossed boats in the bay.
1906 4/18	N. California	4	E	San Francisco	0.1	Recorded.
1927 11/4	<i>C. California EQ off Pt. Arguello</i>	4	<i>E</i>	<i>San Francisco</i>	<i><0.1</i>	<i>Recorded</i>
1992 4/25	<i>N. California M 7.1 Cape Mendocino EQ</i>	4	<i>E</i>	<i>Alameda San Francisco</i>	<i><0.1 <0.1</i>	<i>Recorded</i> "

¹ V - Validity: (Soloviev and Go, 1974; and Cox and Morgan, 1977)

1 = Probably not a valid report

2 = Possibly a valid report

3 = Probably a valid report

4 = Certainly a valid report

² C – Cause of tsunami:

L = Landslide

M = Meteorological

E = Earthquake

³ Topozada et al. 1992

2.2.1 1868 Hayward fault earthquake

The 1868 Hayward Fault earthquake reportedly caused a 6 m (19.7 ft) surge of water at the Cliff House on the NW side of San Francisco, outside the Bay (Lander, 1993). This was attributed to an earthquake-triggered landslide. The accounts of the 1868 event are confusing. A number of vessels reported feeling the earthquake shock but only a few

reported any wave or current activity. Waves were reportedly recorded on a tide gage at Government Island (near Alameda) but the record has been lost. It is unlikely that the 1868 event generated a significant tsunami within the Bay.

2.2.2 1898 Mare Island earthquake

The 1898 Mare Island earthquake produced the largest credible local tsunami wave heights within San Francisco Bay. The 1898 Mare Island earthquake is believed centered on the southern end of the Rogers Creek fault (Toppozada et al., 1992). The Rogers Creek fault is probably the right-stepping continuation of the Hayward fault (Parsons et al., 2003). In a right-lateral strike-slip environment, a right step produces an area of localized extension (Figure 7). Under this model, it is not purely coincidence that the deepest part of San Pablo Bay would be centered over the step-over, since repeated movement on the two faults would cause subsidence in that area.

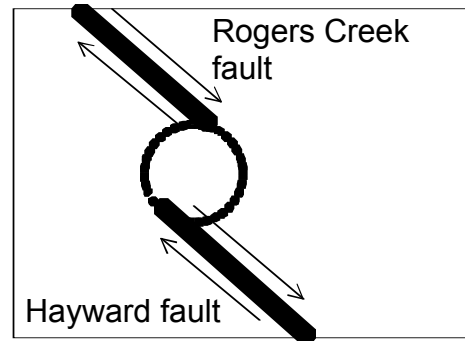


Figure 7 - Right step-over in a right lateral fault system creates a releasing bend and an area of extension and subsidence (dashed circle).

The 1898 Mare Island earthquake produced a tsunami estimated at .6 m (2 ft) at an unspecified location in the Bay (Toppozada et al., 1992). The accounts below (Lander et al., 1993) are typical of the reports:

“...The waters of San Francisco Bay rose in a tidal wave two feet high, but almost immediately subsided.” *The Record Union*

“The water off the Oakland mole (breakwater) was churned into big seas, and the yachts were severely tossed about for several minutes. Large waves beat against the rocking ferry houses but did no damage.” *The San Francisco Call*

Parsons and others (2003) examine the step-over zone between the Rogers Creek and Hayward faults in detail and include numerical modeling of a step-over-induced tsunami that is discussed in section 3 below. They report that historic hydrographic surveys before and after the earthquake suggest subsidence occurred in the step-over region, possibly related to the earthquake.

2.2.3 1906 San Francisco earthquake

A small tsunami was recorded at the Fort Point tide gauge after the April 18, 1906 San Francisco Earthquake. The tsunami was recorded as a 10 cm (4 inch) fall in sea level that began 7 to 10 minutes after the earthquake and lasted approximately 15 minutes. Following this water motion, there was no significant positive wave, but rather a series of two or three more withdrawals with a period of approximately 45 minutes and amplitude

of 5 cm (2 inch) (Lander et al., 1993; Geist and Zoback, 1999). Numerical modeling of the 1906 tsunami by Geist and Zoback (1999), suggest that the tsunami was generated by coseismic subsidence just offshore as the San Andreas fault crosses a short right step offshore of San Francisco.

3. PRIOR RESEARCH ON SAN FRANCISCO BAY TSUNAMIS

Several previous studies have looked at inundation, tsunami heights and estimated recurrence for San Francisco Bay. Ritter and Dupre (1972) mapped areas of potential tsunami inundation within the Bay (Figure 8). They assumed only teletsunami sources and used a water height of 20 feet (6.1 m) at the Golden Gate. This value was chosen because it was the approximate value of peak inundation at Crescent city in 1964. They used Magoon's (1966) attenuation relation to estimate heights of possible flooding throughout the bay. For example, the peak amplitude at Oakland is 3 m (10 ft), at Mare Island 0.6 m (2 ft). They extrapolated Wiegel's (1970) frequency of occurrence graph for San Francisco Bay (Figure 9) to estimate that the mapped inundation (Figure 8) represented a 200-year event. We note that Wiegel's graph is based primarily on five events (1946, 1952, 1957, 1960, 1964) and the slope extrapolated by Ritter and Dupre has been chosen to parallel the Crescent City recurrence graph with no justification.

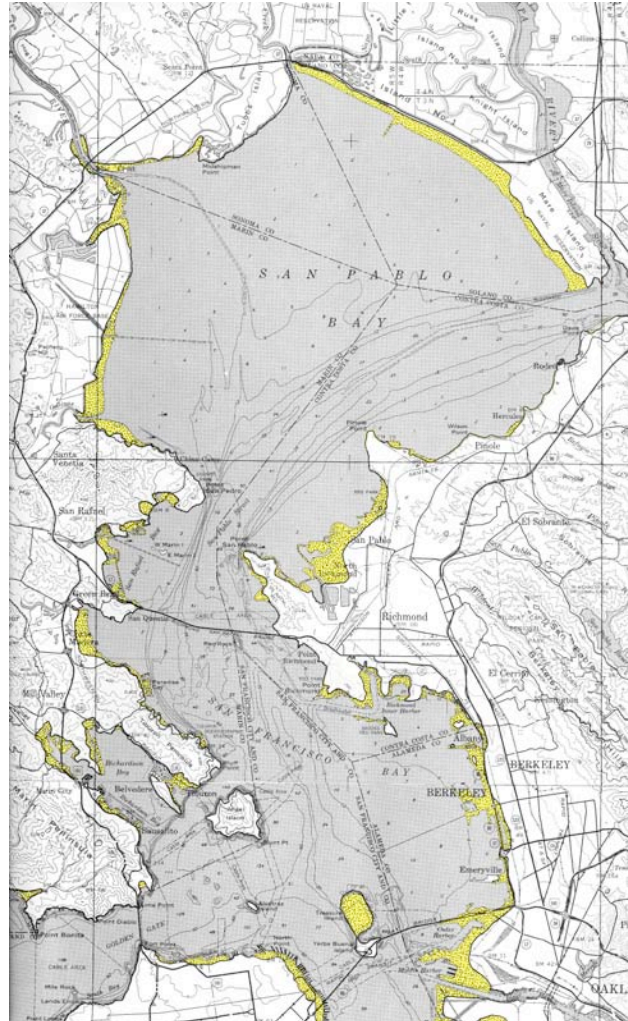


Figure 8 – Areas of potential tsunami inundation (yellow) by a 20 foot tsunami at the Golden Gate (after Ritter and Dupre, 1972).

Garcia and Houston (1975) made 100 and 500-year tsunami predictions for San Francisco Bay for the Federal Insurance Administration as input for a flood insurance study and report. They considered the probabilities of teletsunami sources from Alaska and the Aleutian trench alone, assuming that the 100-year and 500-year events are not strongly affected by events from other regions of the Pacific. They did not address the possibility of locally generated tsunamis. Using a numerical model, they predicted the height of these tsunami waves along the coast of North America as well as inside San Francisco Bay.

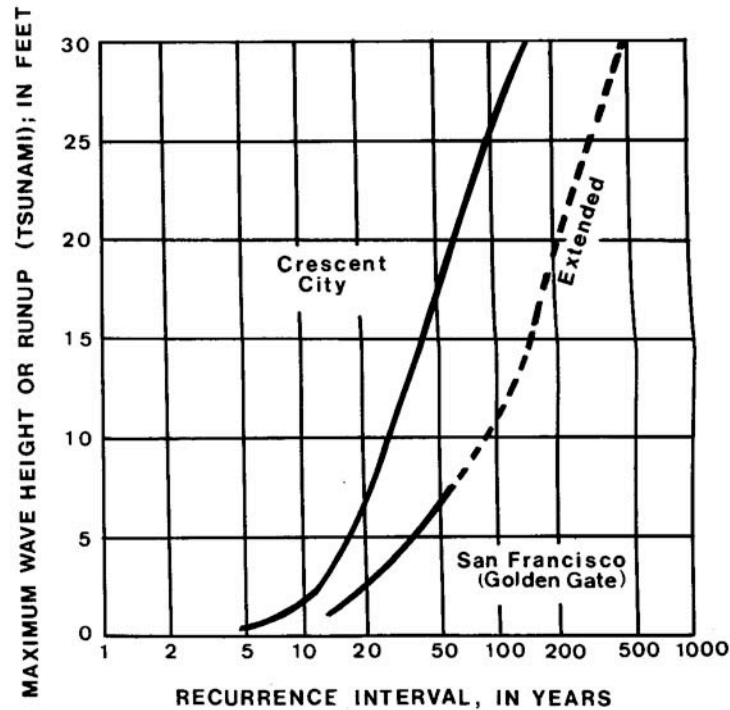


Figure 9 – Frequency of occurrence for maximum tsunami waves at the Presidio in San Francisco based on Wiegel, 1970 and extrapolated by Ritter and Dupre, 1972,

We note that both Garcia and Houston's (1975) 100-year and 500-year values do not mimic the attenuation relation showed by Magoon (1966). Their recurrence estimate for Alaska and Aleutian events was based only on historic events. The mid-20th century may be anomalous for large Alaska tsunamigenic events and these recurrence relationships need to be re-evaluated using the paleoseismic data now available. The restriction of sources to Alaska and the Aleutians also needs to be re-examined particularly in light of the Cascadia Subduction Zone (CSZ) megathrust that is believed to have an approximate 500 year return period and is capable of producing tsunami amplitudes in the source area comparable to 1964 Alaska or 2004 Sumatra. It should also be noted that the Houston and Garcia modeling, while ground breaking at the time, is very crude when compared to the level of sophistication available in modern numerical codes. Houston and Garcia computed tsunami wave amplitudes outside of San Francisco Bay, and then performed their calculations inside the Bay using a forced wave input with the precomputed amplitude and a set period of 38 minutes, a value based on observations after the 1964 Alaskan event. Our method (Section 4) differs in that we consider a wider variety of input sources from subduction zones around the Pacific and we directly compute the tsunami wave effects from source to the study area using the same model.

Eric Geist performed hydrodynamic modeling to examine the tsunamigenic potential of the Hayward – Rogers Creek step-over ((Parsons et al., 2003). Subsidence in the step-over region was modeled as by 0.35 m (1.2 ft) of slip on a high angle 18 km (11.3 miles) wide normal fault. The maximum wave height produced by this model was 0.1 m (.3 ft), well below the reported ~0.6 m (2 ft) height in Bay by the Union Record. It is possible

that the reported 1998 water heights are inaccurate as the event occurred at night and storm activity obscured any recording on the Presidio marigram (Lander, 1993). Geist used a uniform slip distribution and suggests that heterogeneous slip might locally amplify the peak water heights. Geist and Zoback (1999) used a similar method to model the 1906 tsunami as a right step-over offshore of the Golden Gate.

4. NUMERICAL METHOD AND MODEL

Numerical modeling of tsunamis is composed of three parts; generation, propagation and runup. The generation phase involves modeling a geophysical source such as a landslide, earthquake or volcanic eruption into an initial water surface displacement and associated velocity field. The next phase of the problem solves the equations of motion to propagate the initial condition from the source region across the computational domain. Finally the runup phase considers the interaction of the wave front with the shoreline and the propagation over dry land.

For this study we used the numerical model MOST (Method Of Splitting Tsunami), to simulate each of the three processes in the tsunami modeling problem. For wave generation in the fault scenarios, the initial disturbance is assumed to be of tectonic origin. MOST uses a version of Okada's (1985) model for surface deformations due to a fault rupture below the surface of the earth. The resulting deformation on the sea floor is translated directly to the water surface and imposed as an initial condition to the wave propagation part of the process. For wave propagation, MOST solves the 2+1 (two horizontal spatial dimensions plus time) dimension non-linear shallow water wave equations. At the shoreline, MOST employs a moving shoreline algorithm to move the wave front across dry land (Titov and Synolakis, 1998). The MOST code has been extensively tested and validated against laboratory and field data and has been shown to be accurate and reliable across a wide range of spatial dimensions (Titov and Gonzales, 1997). The MOST model is currently in use at NOAA's Pacific Marine Environmental Laboratory as the primary tool for creating tsunami forecasting and hazard assessment tools and in the State of California for producing inundation and evacuation maps.

In addition to faults, one scenario (Farallon Islands) examined the tsunami hazard caused by a submarine landslide. All slides possess the same two basic features: a rupture surface (failure plane) and a displaced mass of material. The displaced material is moved through the acceleration of gravity along the failure plane. A slide that either hits the water from land above (subaerial) or a completely submerged slide can cause a tsunami by displacement of the water volume it moves through. The size of a slump-generated tsunami is related to the volume of displaced material, slip velocity, displacement distance, slope angle and coherence of the slide block. The sliding mass paradigm for modeling submarine landslides is based on the classic work of Wiegel (1955) modified by more recent studies (Raichlin and Synolakis, 2003). We used the same landslide characteristics used in recent studies of the tsunami hazard in the Palos Verdes, CA area (Borrero, 2002). For the initial wave, we assumed a total amplitude of 10 m using an asymmetric dipole shape with 7 m of drawdown and 3 m positive wave and 4 km of mass

displacement. These same conditions produced an initial wave around 8 – 12 m (26 – 39 ft) in Palos Verdes (Bohannon and Gardner, 2004), which is located in shallower water.

4.1 NUMERICAL GRIDS

The numerical grids used in this study were derived from a 3-arcsecond (approximately 75 x 90 m) combined topography and bathymetry grid and designed to capture all potential inputs to the MOT locations (Figure 10, Table 4). The model was set up with a system of three nested grids as shown in Figure 11. The outermost grid was sampled to 30-arcsec, the intermediate grid to 15-arcsec while the full resolution (3-arcsec) data was used for the innermost grid. Model output is designated at the specific MOT locations. Summary tables in Appendix 2 use the location IDs in Table 4.

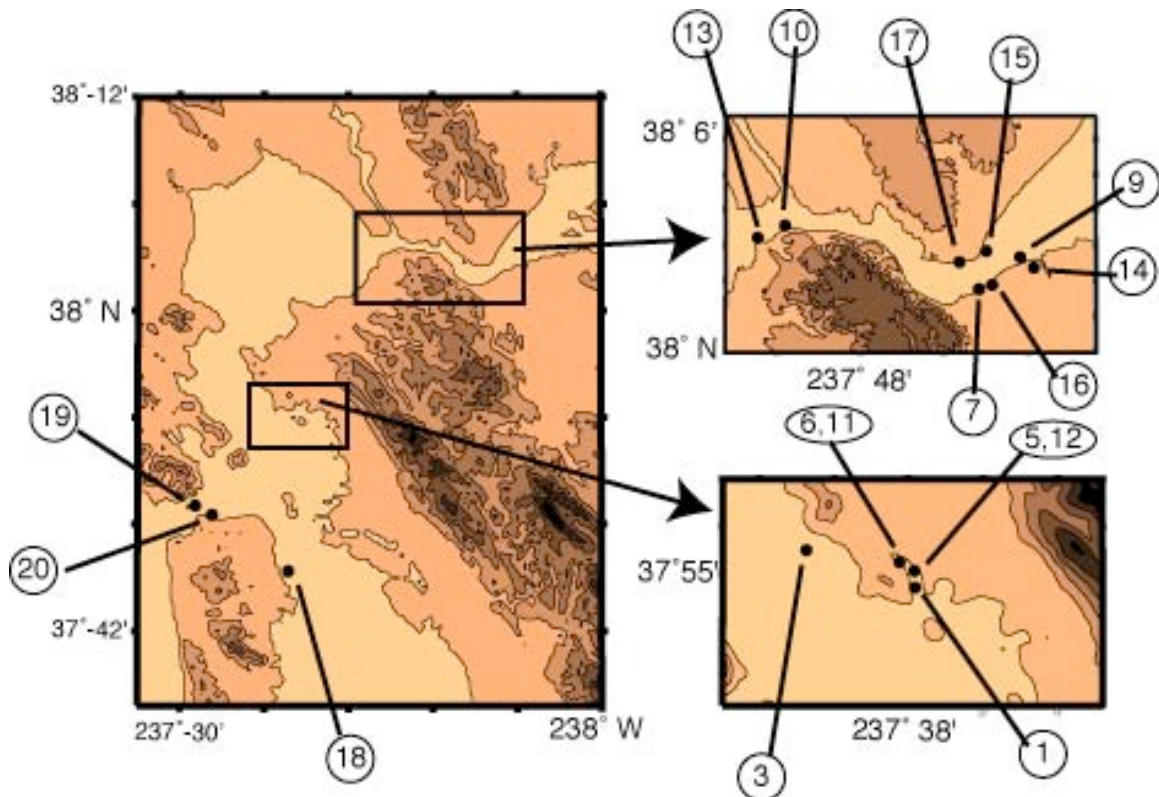


Figure 10 - Locations of Marine Oil Terminals considered in this study (see Table 4). Inner Richmond: locations 5, 6, 11, 12. Outer Richmond: location 3, Carquinez West: locations 10, 13. Carquinez East: locations 7, 9, 14, 15, 16, 17.

Table 4 – San Francisco Bay Area Marine Oil Terminal Locations

ID	Name	Latitude	Longitude
1	BP West Coast Products Richmond	37.9133	237.6342
3	Chevron USA, Inc., Richmond	37.9225	237.5892
5,12	Kinder Morgan and ConocoPhillips, Richmond	37.9167	237.6350
6,11	IMTT and Shore Terminals LLC, Richmond	37.9208	237.6317
7	Shell Oil Products, US, Martinez	38.0325	237.8758
9	Pacific Atlantic Terminals, Martinez	38.0467	237.8983
10	Pacific Atlantic Terminals, Selby	38.0592	237.7592
13	ConocoPhillips, Rodeo Refinery	38.0542	237.7417
14	Tesoro, Inc. - Avon Wharf	38.0492	237.9092
15	Tesoro, Inc. - Amorcio Wharf	38.0350	237.8775
16	Valero Refining Berth 1, Benicia	38.0367	237.8817
17	Valero Refining Berth 2, Benicia	38.0417	237.8600
18	Mirant Potrero LLC, San Francisco	37.7517	237.6317
19	Golden Gate, entrance to San Francisco Bay	37.8150	237.5200
20	The Presidio (Fort Point)	37.8067	237.4167

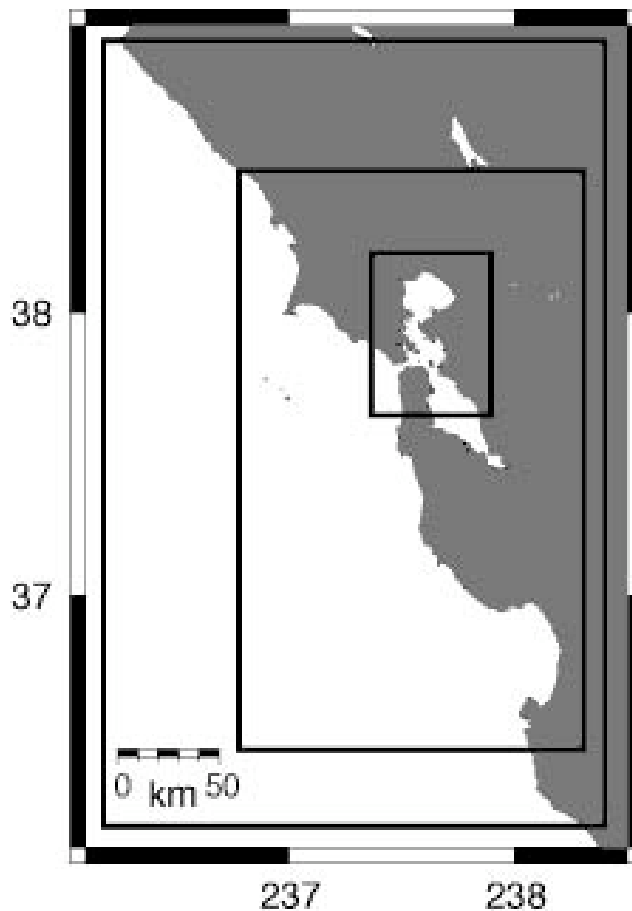


Figure 11 – Coverage areas for the three numerical grid regions.

5. TSUNAMI SOURCES

To investigate the tsunami effects at MOT locations San Francisco Bay, several near- and far-field sources were used. A far-field source is one where the source region is located a great distance from the region considered for the tsunami effects. If the source is an earthquake, this means that the affected area lies outside of the region where ground shaking is felt or where there is coseismic surface deformation. A near-field tsunami on the other hand is one where the tsunami source is close to the area affected, where ground shaking or surface deformation for earthquake sources would be experienced.

In the case of San Francisco Bay, the near-field source region would include faults and landslides inside the bay itself, as well as faults immediately offshore of the mouth of the Golden Gate. Potential far-field sources include large earthquakes on the various subduction zones around the Pacific Rim. This includes events on the Cascadia subduction zone, the Alaska-Aleutian subduction zone, the Kuril Island and Japan subduction zones (Figure 12) and the Chile-Peru subduction zone.

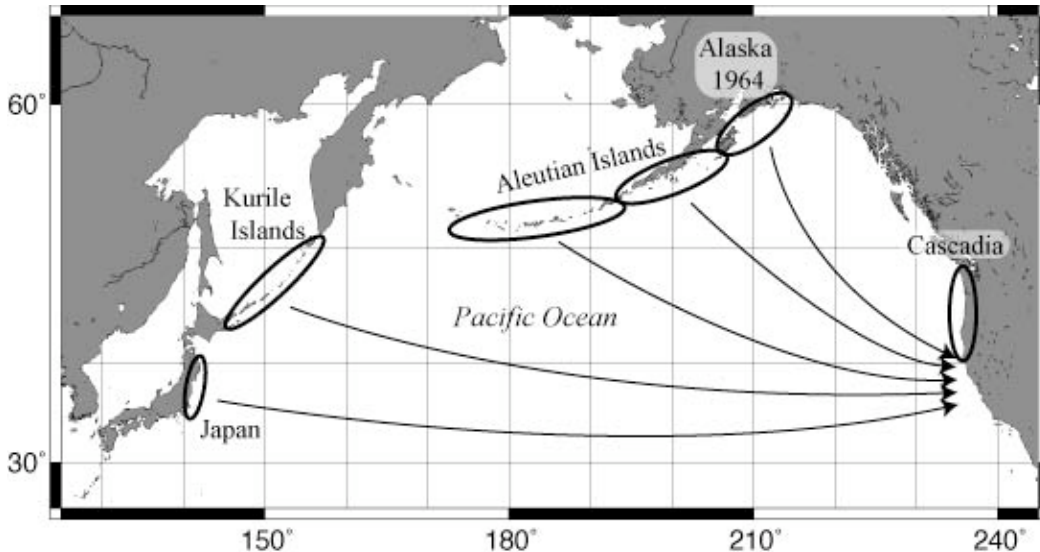


Figure 12 - Source regions in the North Pacific for far field tsunami propagating into San Francisco Bay.

5.1 SUBDUCTION ZONE SOURCES

In order to model the far-field events, we used NOAA's FACTS (Facility for the Analysis and Computation of Tsunami Simulations) database. This database contains the full trans-oceanic simulations for tsunamis generated on segments of the major subduction zones along the Pacific Rim. The database was created by subdividing each subduction zone into 2 parallel rows of 100 km long by 50 km wide fault segments (Figure 13). A pure thrust earthquake mechanism with unit slip (1 m) is then imposed on each segment and the resultant trans-oceanic wave propagation is computed and stored. Larger earthquakes and tsunamis are then created from this database by combining

segments and multiplying the output by an appropriate scalar to reach the desired earthquake magnitude.

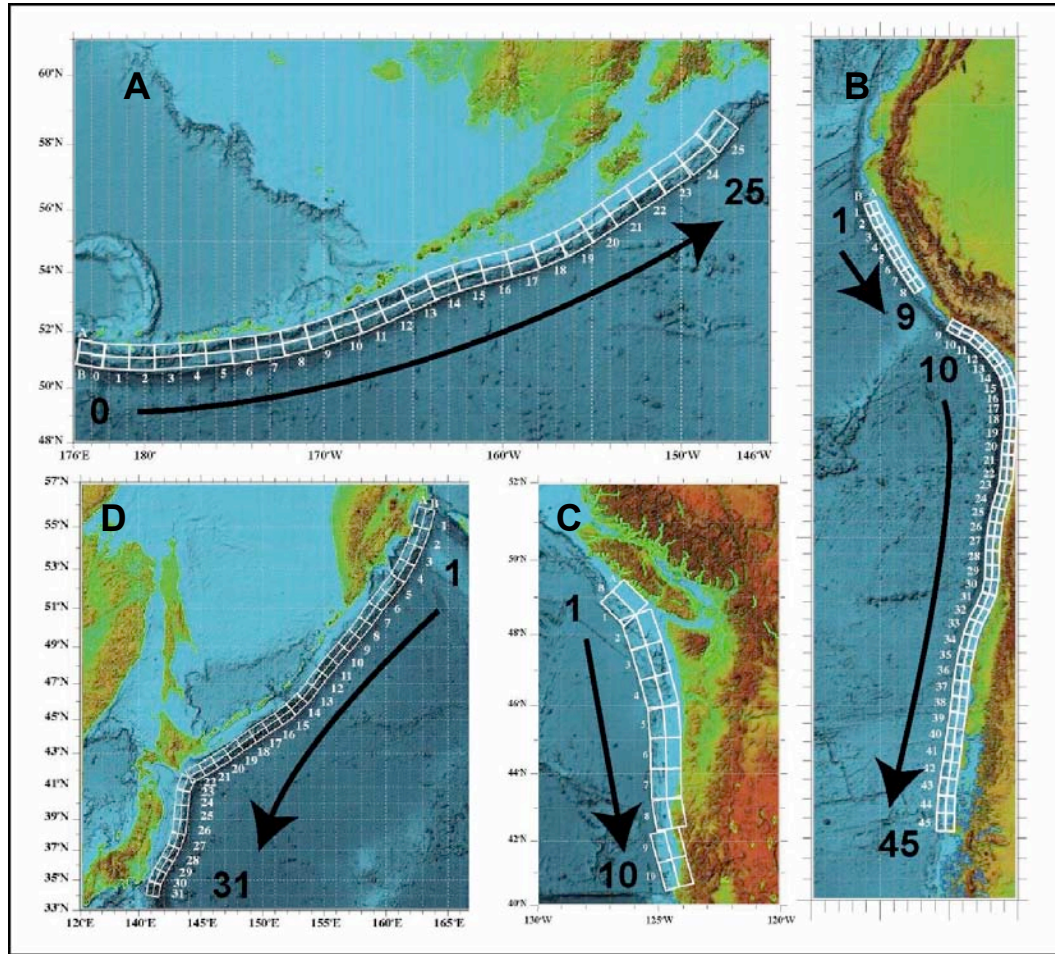


Figure 13 – Subduction zones of the Pacific Rim discretized into 2 parallel rows of 100 km long by 50 km wide fault segments. Clockwise from upper left; A-Alaska-Aleutian Islands, B-South America, C-Cascadia subduction zone, D-Kamchatka-Kuril-Japan subduction zone. Numbers refer to segments in Figure 18.

To calculate M_w , we use the formula: $M_w = 2/3 \log_{10} M_0 - 6.0$ (Yeats et al., 1997), where M_0 is the seismic moment in Nm (Newton meters). The seismic moment is calculated by the formula: $M_0 = \mu u A$ where u is the slip on the fault, A is the area of the fault plane and μ is shear modulus of elasticity of the crust and is taken to be $3 \times 10^{10} \text{ N/m}^2$ (Yeats et al., 1997). Sources can be constructed by adding 100 km long and 50 km wide segments. A magnitude 8.9 earthquake with a fault length of 800 km and a fault width of 100 km (from the two rows of 50 km wide segments) requires an average slip of 9.3 m (30.5 ft) on each fault segment. The computed tsunami from eight adjacent 100 km segments is multiplied by 9.3 and the results linearly combined into one resultant wave field. Times series of wave height and velocity are interpolated at the boundary of the outermost local grid (see Figure 11) and used as the initial condition to the local tsunami inundation model (Borrero et al., 2004). A summary of all the fault scenarios used in this study is given in Table 5.

$M_w = 2/3 \log_{10} M_o - 6.0$ where:

$M_o = \mu u A$, $A = L \times W$, $\mu = 3 \times 10^{10} \text{ N/m}^2$

Example: $M_w = 8.9$, $L = 800 \text{ km}$ and $W = 100 \text{ km}$

Find displacement on the fault (u) in meters.

$(8.9 + 6.0) (3/2) = \log_{10} M_o$

$M_o = 2.24 \times 10^{22} \text{ Nm}$

$M_o = \mu u A$

$2.24 \times 10^{22} \text{ Nm} = (3 \times 10^{10} \text{ N/m}^2) (8 \times 10^5 \text{ m}) (1 \times 10^5 \text{ m}) (u)$

$u = 9.3 \text{ m}$

Equation 1 – Sample calculation for determining average fault slip from a given moment magnitude and fault geometry

Composite Tsunami Source Name	L (km)	W (km)	slip (m)	dip deg	rake deg	strike deg	depth (km)	Mo (Nm)	M _w
Alaska 1964								7.80E+22	9.26
Segment 1	400	200	10	10	90	218	5		
Segment 2	300	300	20	9	75	241	15		
Aleutian I	500	100	10	15	90	n/a	5	1.50E+22	8.78
Aleutian II	500	100	10	15	90	n/a	5	1.50E+22	8.78
Aleutian III	700	100	25	15	90	n/a	5	5.25E+22	9.15
Kuril I	1000	100	9	15	90	n/a	5	2.70E+22	8.95
Kuril II	400	100	10	15	90	n/a	5	1.20E+22	8.72
Kuril III	400	100	10	15	90	n/a	5	1.20E+22	8.72
Kuril IV	400	100	10	15	90	n/a	5	1.20E+22	8.72
Japan I	900	100	5	15	90	n/a	5	1.35E+22	8.75
Japan II	400	100	10	15	90	n/a	5	1.20E+22	8.72
Chile 1960	1000	100	20	15	90	n/a	5	6.00E+22	9.26
Chile 1960W	1000	200	23	15	90	n/a	5	1.38E+23	9.43
Chile North	1400	100	25	15	90	n/a	5	1.05E+23	9.35
Cascadia I	600	100	10	15	90	n/a	5	1.80E+22	8.84
Cascadia II	800	100	11.1	15	90	n/a	5	2.70E+22	8.95
Cascadia III	1200	100	20	15	90	n/a	5	5.76E+22	9.17
Cascadia SN	-	-	-	-	-	-	-	4.61E+21	8.4
Segment 1	150	80	8	10	90	350	5		
Segment 2	90	80	8	10	90	340	5		
Cascadia SW	-	-	-	-	-	-	-	5.76E+21	8.5
Segment 1	150	100	8	10	90	350	5		
Segment 2	90	100	8	10	90	340	5		
Cascadia SP2	-	-	-	-	-	-	-	5.54E+21	8.5
Segment 1	150	100	8	10	90	350	5		
Segment 2	90	30	4	10	90	340	5		
Segment 3	90	70	8	10	90	340	10		
Segment 4	90	10	4	20	90	310	5		
Hayward-Rodgers Creek	10	18	1.5	70	-90	40	5	8.10E+18	6.61
San Gregorio	50	15	2	60	90	320	5	4.50E+19	7.10

Table 5 - Summary of source parameters used for each fault scenario. Strike values for the far-field sources derived from the FACTS database are listed as 'n/a' since they are dependent on the local curvature of the subduction zone.

5.1.1 Cascadia subduction zone

The Cascadia subduction zone (CSZ) (see Figures 12 and 13) is the boundary between the Pacific and North American tectonic plates along the Pacific Northwest margin of North America. The CSZ extends along the Pacific coast of North America from Cape Mendocino, California to Vancouver Island, British Columbia in Canada. The CSZ is believed to produce infrequent earthquakes of magnitude 8.5 or larger, with the most recent in 1700 A.D. rupturing the entire zone (Satake et al., 2003). We modeled several variations of earthquakes on the CSZ ranging in magnitude from 8.4 to 9.2. The source parameters are summarized in Table 5.

***Cascadia I* $M_w = 8.84$** – A total fault length of 600 km (375 miles) with a slip of 10 m (33 ft). This represents a rupture on the northern portion of the fault extending from Newport, Oregon to the middle of Vancouver Island Canada.

***Cascadia II* $M_w = 8.95$** – For this scenario we modeled an earthquake starting at the California – Oregon Border and rupturing to the north to the middle of Vancouver Island over a fault length of 800 km (500 miles) with an average slip of 11 m (36 ft).

***Cascadia III* $M_w = 9.17$** – For this scenario we modeled the largest credible rupture extending 1200 km (750 miles) from Cape Mendocino, California to Vancouver Island, British Columbia with an average slip of 20 m (65 ft). This is comparable to the December 26, 2004 Sumatra rupture.

Cascadia subduction zone southern segments – For the southern segments of the Cascadia subduction zone, we used three previously published source models (***Cascadia***, ***SN***, ***Cascadia SW***, ***Cascadia SP2***) described in (Bernard et al., 1994).

***Cascadia SN* $M_w = 8.4$** – This is a 2-fault scenario with a total fault length of 240 km (150 miles) and a fault width of 80 km (50 miles) and average slip of 8 m (26 ft) on each segment.

Cascadia SW* $M_w = 8.5$** – This scenario is identical to ***Cascadia SN except with a width of 100 km (62 miles) as opposed to 80 km (50 miles).

***Cascadia SP2* $M_w = 8.5$** – This scenario considers slip partitioning on a more steeply dipping fault, the Little Salmon Fault, which lies above the main subduction interface in the accretionary wedge just south of Humboldt Bay, California. Seismic moment is conserved for this scenario and the total slip on the southern segment is reduced to compensate for the additional slip on the splay fault.

5.1.2 Alaska and the Aleutian Islands

Four sources were used to investigate the effects of tsunamis originating in Alaska and the Aleutian Islands. These include a scenario based on the March 28, 1964 Great

Alaskan earthquake, two hypothetical magnitude 8.8 events in the central part of the Aleutian Islands as well as a magnitude 9.15 event in the central Aleutians.

1964 Alaska $M_w = 9.26$ – The fault model for this scenario was created by NOAA-PMEL and based on investigations by Plafker (1972) and Johnson et al., (1996). They used two fault planes to model the deformation field resulting from the earthquake. The smaller, western plane had dimensions of 400 x 200 km (250 X 125 miles) and an average slip of 10 m (33 ft). The second fault plane to the east measured 300 x 300 km (190 X 190 miles) with an average slip of 20 m (66 ft).

Aleutian I $M_w = 8.78$ – Located west of the 1964 rupture and extending 500 km (312 miles) from Kodiak Island to the Alaska Peninsula, average slip of 10 m (33 ft).

Aleutian II $M_w = 8.78$ – Located west of Aleutian I, extending from the central Alaska Peninsula Island to Unimak Island with the same length and slip as Aleutian I.

Aleutian III $M_w = 9.15$ – This scenario was created to investigate the effects of a ‘worst case’ type scenario and combines the rupture in the two previous scenarios. An 800 km (500 mile) long fault with 25 m (82 ft) of slip was located in the region along the Aleutian Subduction Zone that was most likely to generate the strongest response within San Francisco Bay. The rupture extends from Kodiak Island to Unimak Island.

Numerous large ruptures have occurred along the central and western portions of the Alaska – Aleutian subduction zone in historic times and the Andreanof and Rat Island segments are capable of producing earthquakes in the upper 8 to lower 9 magnitude range. However, the arc in these areas is not directed favorably towards the west coast of the United States and even great earthquakes will not impact San Francisco Bay as significantly as the Aleutian III case.

5.1.3 Kuril Islands

Large earthquakes have occurred on the Kuril – Kamchatka Subduction Zone resulting in trans-pacific tsunamis. Two events in 1923 and one in 1952 were observed along the US west coast. The earthquakes had magnitudes of 8.3 (February 3, 1923), 7.2 (April 13, 1923) and 8.2 (November 4, 1952). For this study we used four different source models. **Kuril I** used a 1000 km (625 mile) long fault and an average of 9 m (29.5 ft) of slip for a magnitude 8.95 event. Three smaller scenarios (**Kuril II, III and IV**) were also simulated using a 400 km (250 mile) fault length and 10 m (33 ft) of average slip. The three smaller scenarios, each with $M_w = 8.72$, were placed at different locations along the Kuril trench to investigate the effect of location on the response within San Francisco Bay.

5.1.4 Japan

Large earthquakes off the coast of Japan have been responsible for numerous large tsunamis in Japan and several trans-pacific events. In particular, the Sanriku earthquake on June 15, 1896, which generated maximum local tsunami runup between 25 and 38 m

(82 to 125 ft) (Lander et al., 1993; Tanioka and Satake, 1996), produced a small tsunami in Sausalito. Tanioka and Satake studied this event and fixed the source parameters based on matching tsunami wave forms recorded at tidal stations to synthetic waveforms generated by numerical simulations. Other researchers (Aida, 1997) have also modeled the faulting characteristics for this event. It should be noted that the slip distribution and fault location between the various studies are quite different, for example Tanioka and Satake (1996) assume 5.7 m of slip over the fault while Aida (1997) assume more than 12 m. *Japan I* used a 900 km (560 miles) fault with 5 m (16.5 ft) of slip and a total moment magnitude of 8.75. A second scenario (*Japan II*) assumed a fault length of 400 km (250 miles) and a slip of 10 m (33 ft) resulting in a $M_w = 8.72$ event.

5.1.5 South American subduction zone

In addition to the cases mentioned above we modeled two scenarios based on sources along the Peru-Chile subduction zone. The first scenario, *Chile 1960* modeled a source similar to the 1960 earthquake. This source used a total fault length of 1000 km (655 miles) and 20 m (66 ft) of displacement for a magnitude 9.26 event. A second scenario *Chile 1960W* models the 1960 event using a wider fault (200 m) and 23 m (75 ft) for a moment magnitude of 9.43, closer to the accepted 9.5 value for this event. A third scenario, *Chile North* used 1400 km (875 miles) of total fault length and 25 m (82 ft) of displacement to simulate an extremely large, $M_w = 9.35$, event on the northern section of the subduction zone.

Great earthquakes have also occurred on the Peru segment of the subduction zone. But these events are less favorably oriented to San Francisco Bay than the events further to the south and were not modeled.

5.2 NEAR-FIELD SOURCES

Near-field sources are underwater faults that might generate vertical deformation within the Bay or immediately adjacent to the Golden Gate or sites with the potential to produce large submarine or subaerial landslides. For faults, we calculate the seafloor displacement due to an earthquake using the elastic dislocation model based on the theory of Okada (1985). This tectonic displacement is then translated directly to the water surface as a static initial condition and allowed to propagate as a gravity wave. The details of each earthquake scenario and the faulting parameters used for the elastic dislocation model are listed in Table 5, as well as in Appendices 1 and 2. The precise location of

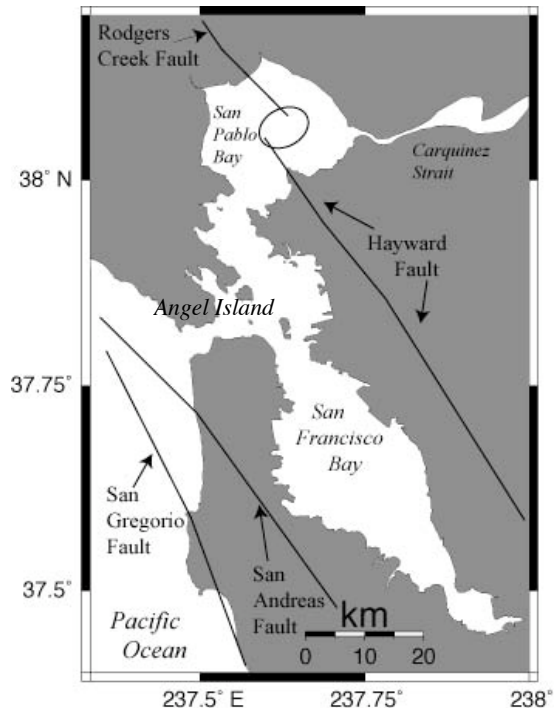


Figure 14 - Location of potentially tsunamigenic faults and slides in the vicinity of San Francisco Bay. The Farallon Islands are offshore, 35 miles west of the Golden Gate.

each source is shown in Appendix 1 along with a plot of the computed maximum wave height across the Pacific Basin and a plot of maximum computed wave height for San Francisco Bay.

Several local sources were considered in order to assess the tsunami hazard in San Francisco Bay. A 1999 USGS study placed a 10 to 30% probability of a magnitude 6.7 earthquake or greater in 30 years on any of three potentially tsunamigenic faults near San Francisco Bay (Working Group, 1999). The probability was listed as 10% for the offshore segment of the San Gregorio Fault, 21% for the offshore strand of the San Andreas Fault and 32% for the Rogers Creek Fault running through San Pablo Bay (Figure 13).

In addition to regional faults, we also examined the potential tsunami hazard caused by submarine or subaerial landslides. We examine potential areas of large slope instabilities within the Bay and adjacent to the Golden Gate.

5.2.1 San Gregorio fault

The San Gregorio fault is part of a system of offshore faults that parallel the coast from Point Arguello north to Bolinas Bay. Just west of San Francisco, the San Gregorio fault converges with the San Andreas Fault in a region of complex faulting which includes several other parallel fault strands including the Golden Gate fault and the Potato Patch fault (Bruns et al., 2002). These fault strands trend northwest and merge on shore as the northern segment of the San Andreas fault. Though it is believed to be predominantly strike-slip in nature, the fault does exhibit reverse faulting characteristics (USGS fault data base, Bruns et al (2002)) in an area west of the northern segment of the San Gregorio Fault known as the San Gregorio Structural Zone. In order to place an upper bound on the tsunamigenic potential of this fault, we model a large ($M_w = 7.1$) thrust mechanism earthquake with a fault length of 50 km (31 miles) that traverses the bight west of the entrance to San Francisco Bay. The detailed fault parameters for this scenario are listed in Table 5.

5.2.2 Hayward – Rodgers Creek fault step-over

Beneath San Pablo Bay is a step-over between the right lateral Hayward and Rodgers Creek faults (Figure 14). The details of this step-over were studied by Parsons et al. (2003). They contend that the Hayward – Rodgers Creek fault step-over is the source for the 1898 Mare Island earthquake and tsunami. They model the tsunami using slip mechanism on a normal fault which steps over from the Hayward to the Rodgers Creek fault. Their simulations were for an earthquake with an approximate magnitude of 6.0, which translates to 0.35 m (1 ft) of slip on a fault plane 6 km (4 miles) long by 18 km (11 miles) wide. Their simulations produce only 0.1 m (4 inch) tsunami waves, in contrast to the 0.6 m (2 ft) reported in historical accounts. We use similar fault geometry but apply more slip to again place an upper bound on the tsunami waves and currents that could be generated by such a mechanism. Our simulation uses a slip of 1.5 m (4.9 ft) resulting in a moment magnitude (M_w) of 6.61.

5.2.3 Landslide on the Farallon Islands

The Farallon Islands are a rocky archipelago 45 to 65 km (28 to 40 miles) offshore of the Golden Gate. The Farallons sit on the continental slope; the easternmost island sits in about 150 m (82 fathoms) water depth which quickly deepens to over 3000 m (1640 fathoms) only 5 miles to the southwest. The sea floor around the diorite islands is littered with the debris of submarine slides and debris flows ranging in scale from a few square meters to hundreds of square meters (Karl and Schwab, 2001). We modeled the largest credible landslide on the east slope of the easternmost island using the same parameters as the Palos Verdes slide (Borrero, 2002).

5.2.4 Other sources

We considered other potential local tsunami sources including slumps and landslides inside the Bay and excitation of seiche by earthquake surface waves. The topography on the Bay margins is generally gentle (Figure 1) and while landslides are common on steeper slopes, there is no history of large volume failures into the Bay. Most of the Bay is very shallow and even if a large slide were to enter the Bay, the volume of water displaced would be small. We briefly examined the only three sites within the Bay that may have tsunamigenic landslide potential to impact the MOT locations: Angel Island, the Golden Gate and the Carquinez Straits.

Angel Island is a 740-acre island in the central San Francisco Bay located 5 km (3 miles) north of San Francisco and 1.6 km (1 mile) southeast of Tiburon (Figure 14). The island is composed primarily of highly fractured Franciscan formation greywacke sandstones and greenstones, reaches an elevation of 238 m (781 feet) and is characterized by slope steepness in the 50 to 75% range (Olivia Chen Consultants, 2003). Although the island sits in a deeper than average part of the Bay, water depths are still less than 50 meters (27 fathoms) in areas any slides might reach. And while slope failures are common on the island, there is no evidence of failures on the scale of hundreds of meters. Any slide-caused tsunami from Angel Island would be small and quickly dissipate offshore and pose no hazard to the MOT locations.

The Golden Gate is a steep gorge cut into Franciscan greywacke, chert and greenstone that separates San Francisco from Marin County. The Bay reaches its maximum depth of 109 m (60 fathoms) in the Golden Gate. Only the headlands on the north side are steep enough to pose any slide hazard into the Bay and historically slides in this area have been small and few (Wentworth et al., 1997). There is no credible basis to support a large slide in this area.

The Carquinez Strait connects San Pablo Bay to Suisan Bay (Figure 14). Only the western end is steep enough to pose slide hazards. The Strait is less than a kilometer wide (.6 mile) and no deeper than 30 meters (16 fathoms). The landslide hazard is not mapped as high (Wentworth et al., 1997) and is not capable of posing a tsunami hazard comparable to the other sources examined in this study.

Seiches generated by earthquake surface waves have been known to produce tsunamis in closed bodies of water and bays (Barberopoulou et al., 2003). The large amplitude surface waves are believed amplified by basin geometry, exciting water oscillations or seiches. To produce significant seiching in a body of water, the forcing periods must be close to the natural period of the bay or one of the overtones. The characteristic periods and overtones for San Francisco Bay are much longer than surface wave periods and we do not consider non-tsunami induced seiches in San Francisco Bay to pose a hazard comparable to the other sources modeled in this study.

6. RESULTS AND DISCUSSION

Detailed plots of the numerical output from each scenario are given in Appendix 1 and a summary of peak positive and negative wave heights, current velocity and direction is given in Appendix 2. Table 6 summarizes peak water heights generated by the 23 scenarios at four locations.

Table 6 - Scenario Water Height Summary

SCENARIO	Mag	Golden Gate	Presidio	Outer Richmond	Inner Richmond	Carquinez
Alaska 1964	9.26	2.58	1.63	0.96	1.31	0.37
Aleutian I	8.78	2.09	1.34	0.90	1.13	0.31
Aleutian II	8.78	1.30	0.90	0.46	0.68	0.23
Aleutian III	9.15	5.35	2.90	1.56	1.59	0.54
Kuril I	8.95	0.32	0.28	0.31	0.62	0.09
Kuril II	8.72	0.20	0.32	0.12	0.24	0.07
Kuril III	8.72	0.47	0.27	0.26	0.56	0.07
Kuril IV	8.72	0.60	0.39	0.21	0.36	0.12
Japan I	8.75	0.24	0.25	0.22	0.49	0.04
Japan II	8.72	0.60	0.39	0.21	0.43	0.08
Chile 1960	9.26	0.61	0.39	0.21	0.43	0.08
Chile 1960W	9.43	1.34	0.78	0.42	0.82	0.17
Chile North	9.35	0.87	0.64	0.49	0.73	0.19
Cascadia I	8.84	0.54	0.34	0.26	0.55	0.14
Cascadia II	8.95	0.58	0.38	0.27	0.49	0.14
Cascadia III	9.17	1.39	1.39	0.67	0.87	0.22
Cascadia SN	8.40	0.45	0.29	0.15	0.28	0.08
Cascadia SW	8.50	0.42	0.26	0.14	0.24	0.06
Cascadia SP2	8.50	0.35	0.27	0.12	0.23	0.07
Hayward-Rodgers Creek	6.61	0.00	0.01	0.00	0.02	0.02
San Gregorio	7.10	0.60	0.40	0.26	0.42	0.11
Farallons	landslide	0.74	0.15	0.08	0.21	0.01

Columns: Mag - earthquake magnitude. Golden Gate – entrance to the Bay, ID 19. Presidio – the Presidio tide gauge location, ID 20. Outer Richmond – offshore Richmond, ID 3. Inner Richmond – inside the Richmond channel, ID 5&12. Carquinez - western entrance of the Carquinez Straits, ID 10.

The largest amplitude waves are generated by Aleutian III scenario followed by Alaska 1964. Both are discussed further in section 6.3 below. Cascadia III produces a 1.4 m

peak wave at the Presidio, larger than any historic event except the 1964 tsunami. This event could cause some damage to boats and floating structures in the Bay, especially if coincident with high tide, but the impacts should be slightly less than 1964. A Cascadia tsunami will cause major damage along the northern California, Oregon and Washington coasts but the San Francisco Bay area is favorably oriented parallel to the strike of the fault zone. Our modeling results are supported by field observations from the Indian Ocean tsunami that show wave amplitudes on the Sumatra coast decaying rapidly south of Meulaboh (Jaffe et al., in press 2006), in coastal areas with a similar location and orientation as San Francisco relative to Cascadia.

The three local sources produce very small waves inside the Bay. The Hayward-Rogers Creek step-over produces a peak height of 0.2 meters in the Carquinez Strait and in the Inner Richmond waterway, larger than the 0.1 m heights in Parsons et al. (2003) but still significantly less than 0.6 m estimated from the few available eyewitness accounts. The San Gregorio event produces slightly larger waves at Inner Richmond (0.4 m) but still much less than the larger teletsunami events. The Farallon landslide produces a negligible wave within the Bay. At the entrance to the Bay, the San Gregorio and Farallon landslide scenarios produce localized water heights comparable to the South American and northeastern Pacific subduction zones, but the volume of water displaced by these local scenarios is much smaller and translates into very small tsunami heights at the MOT locations.

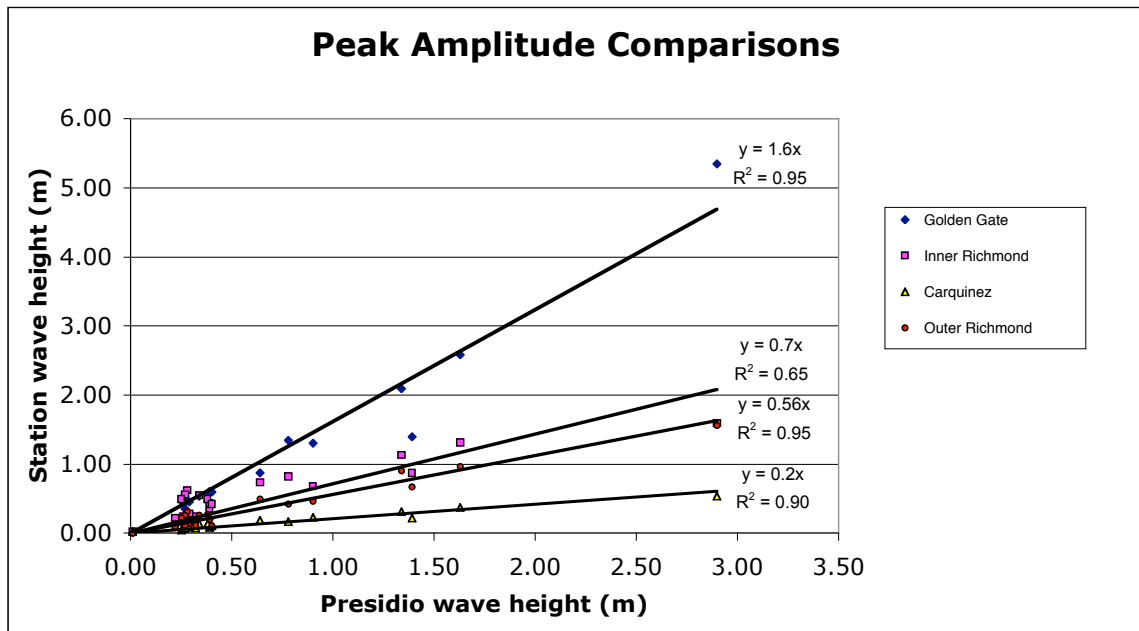


Figure 15 – Comparison of peak water height to Presidio tide gauge site for locations in Table 6. Linear trends for each data set given with R^2 regression values.

Figure 15 compares the peak positive water height value at the Golden Gate, Outer and Inner Richmond, and Carquinez locations (Table 6) to the Presidio tide gauge site. The amplitudes of each site show a rough linear relationship to the Presidio values. Presidio water heights average just over 60% of the water heights at the entrance to the Bay (Golden Gate). The Outer Richmond values are about 56% of the Presidio water heights, very close to the 50% attenuation Magoon (1966) estimates from 1960 and 1964

marigrams (see Figure 6). At the Carquinez locations, water heights are 20% or less of the Presidio values. The Inner Richmond sites show the most complexity, always larger than Outer Richmond and averaging 70% of the Presidio values. But the regression fit is not nearly as good as at the other sites, suggesting complex amplification within the narrow Richmond Channel.

6.1 COMPARISON TO HISTORICAL DATA.

To check the validity of our model and method, we first compared the model results of simulated historic events to available instrumental records. Tide gauge recordings from inside San Francisco Bay allow for a direct comparison of the modeled to observed wave behavior. Fortunately marigrams exist for the 1960 and 1964 tsunamis in San Francisco Bay.

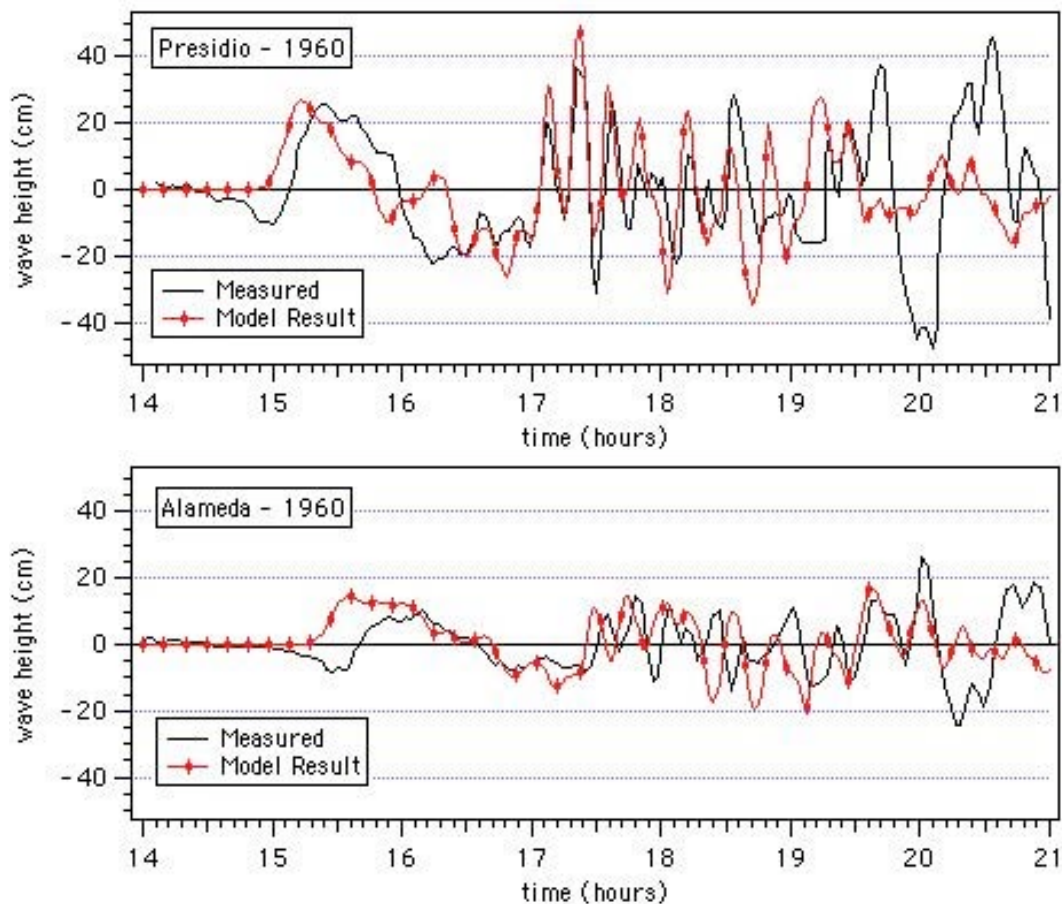


Figure 16 – Modeled vs. recorded time series of water levels at The Presidio and Alameda for the 1960 Chilean tsunami.

Figure 16 shows a comparison between the modeled and recorded wave heights for the 1960 tsunami at the Presidio, just inside the entrance to San Francisco Bay and at Alameda on the eastern shore of the Bay. The agreement between the model and the tide gauge data is remarkable in terms of amplitude and period. There is some discrepancy in the modeled arrival time, however it is only about 7 minutes and is negligible when compared to more than 14 hours of propagation time required for the waves to travel

from South America and reach the entrance of San Francisco Bay. Our model assumes an instantaneous rupture and displacement at the earthquake source, when in fact earthquakes of this size may take five minutes or longer to rupture the complete fault zone, which may explain a large part of the discrepancy. Tsunami travel time is also affected by the shallow water bathymetry in the earthquake source region and the deep ocean bathymetry along the tsunami travel path, neither of which are known perfectly. Our model captures the initial wave form and the first several hours of the 1960 tsunami quite well, but does not reproduce the large amplitude oscillations which begin some 5 hours after the first wave arrival and persist for over 3 hours (see Figures 4 and 16). The exact cause for these late arriving waves has not been explained in the literature, however it could be a resonance effect of the Bay as proposed by Wiegel (1970), an amplified response of the tide gauge itself or some combination of the two.

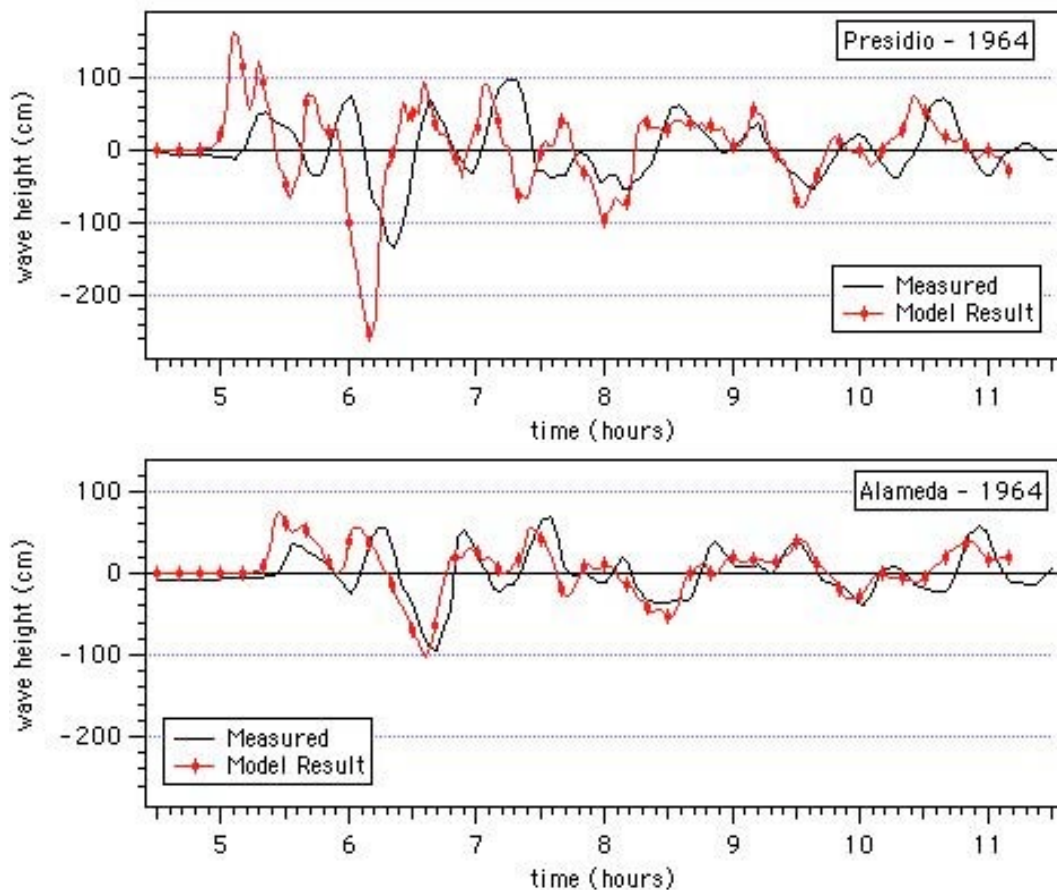


Figure 17 – Modeled vs. recorded time series of water levels at The Presidio and Alameda for the 1964 Alaskan tsunami.

A comparison of recorded and modeled wave heights for the 1964 event is shown in Figure 17. While the model over-predicts the initial wave peak and first large withdrawal, especially on the Presidio tide gauge, the amplitudes and periods of the subsequent peaks match quite well. There is a slightly larger discrepancy in arrival times, approximately 15 minutes, than in the 1960 case. Again we consider this negligible in terms hazard assessment at the MOT sites. The good fit of the model data to the tide

gauge recordings gives us confidence in the model and provides a strong foundation for investigating the relative influence of different far field sources.

6.2 EFFECT OF SOURCE REGION.

Using the FACTS database, we investigated the effect of the location of the tsunami source region on the wave height offshore of the entrance to San Francisco Bay. This was done by comparing the maximum computed wave height from each of the unit sources in the FACTS database (Figure 13).

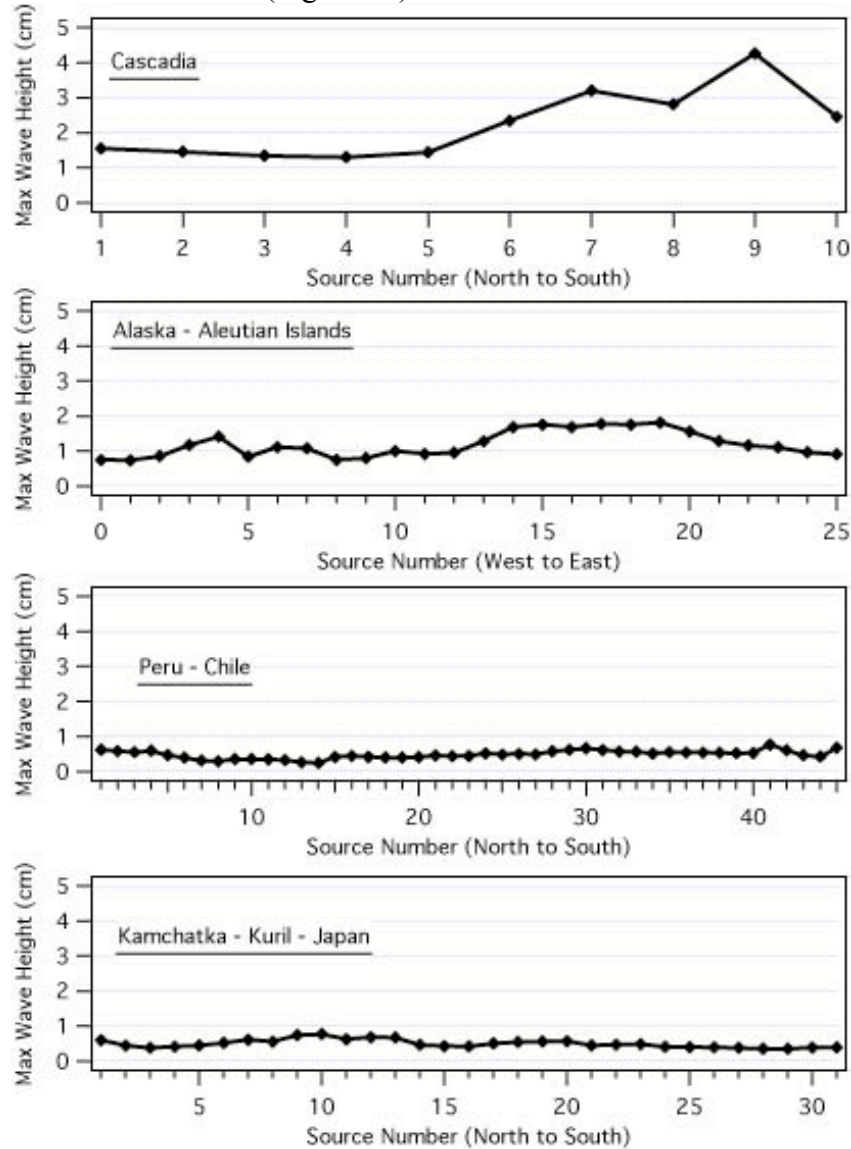


Figure 18 – Computed tsunami wave height at 37.7° N, 122.67° W (offshore of the entrance to San Francisco Bay) from individual unit (1-m) slip sources along four different subduction zones. Note, each slip source is the same length.

The resulting plots are shown in Figure 18. It appears that the largest response is from Cascadia. However, the response is at an offshore location, about 21 km (13 miles) west

of the Golden Gate, and only the 5 southern segments produce amplitudes of over 1.5 cm. The Cascadia segments are directed strongly towards the southwest (see Appendix 1, p. 81) and not towards San Francisco Bay. This is reflected in their relatively small wave amplitudes for Cascadia scenarios at the MOT locations within the Bay (Figure 19). Eight of the Alaska -Aleutian slip sources produce 1.5 cm or larger responses, especially segments 14 through 19 (See Figure 13), and they are directed towards the Bay.

Scenario Name	Number
Cascadia SN	1
Cascadia SP2	2
Cascadia SW	3
Cascadia I	4
Cascadia II	5
Cascadia III	6
Alaska 1964	7
Aleutian I	8
Aleutian II	9
Aleutian III	10
Kuril I	11
Kuril II	12
Kuril III	13
Kuril IV	14
Japan I	15
Japan II	16
Chile 1960	17
Chile 1960W	18
Chile North	19

Table 7 – Numbers of composite sources (Table 5) referenced in Figure 19 and Appendix 1.

To investigate the sensitivity of the response at each MOT location, we plotted the maximum wave height and drawdown at terminal locations for each of our tsunami sources (Figure 19). The sources are arranged in geographical order from east to west starting with Japan, followed by Kurils, Alaska, Cascadia and South America and assigned a number (Table 7). It is evident that that strongest response occurs at MOT locations in the Richmond area from sources in Alaska and the Aleutian Islands. The longest rupture of the Cascadia subduction zone produces the next largest response, producing peak heights and drawdowns close to 1 m at the MOT locations. While slightly larger than South America and the northwestern Pacific sources, this suggests that the CSZ is not the dominant player for tsunami hazards within the Bay. While great earthquakes on the CSZ will produce significant and damaging runup elsewhere, our modeling shows that most of this energy is radiated offshore towards Hawaii and Japan and relatively little wave energy is propagated south along the coast. This is also shown in the maximum trans-pacific wave height plots for the Cascadia subduction zone cases in Appendix 1. The smaller ruptures of the CSZ pose very little hazard in San Francisco

Bay. The largest South American sources are slightly smaller than Cascadia III with much smaller response seen for sources in the Kuril Islands and Japan.

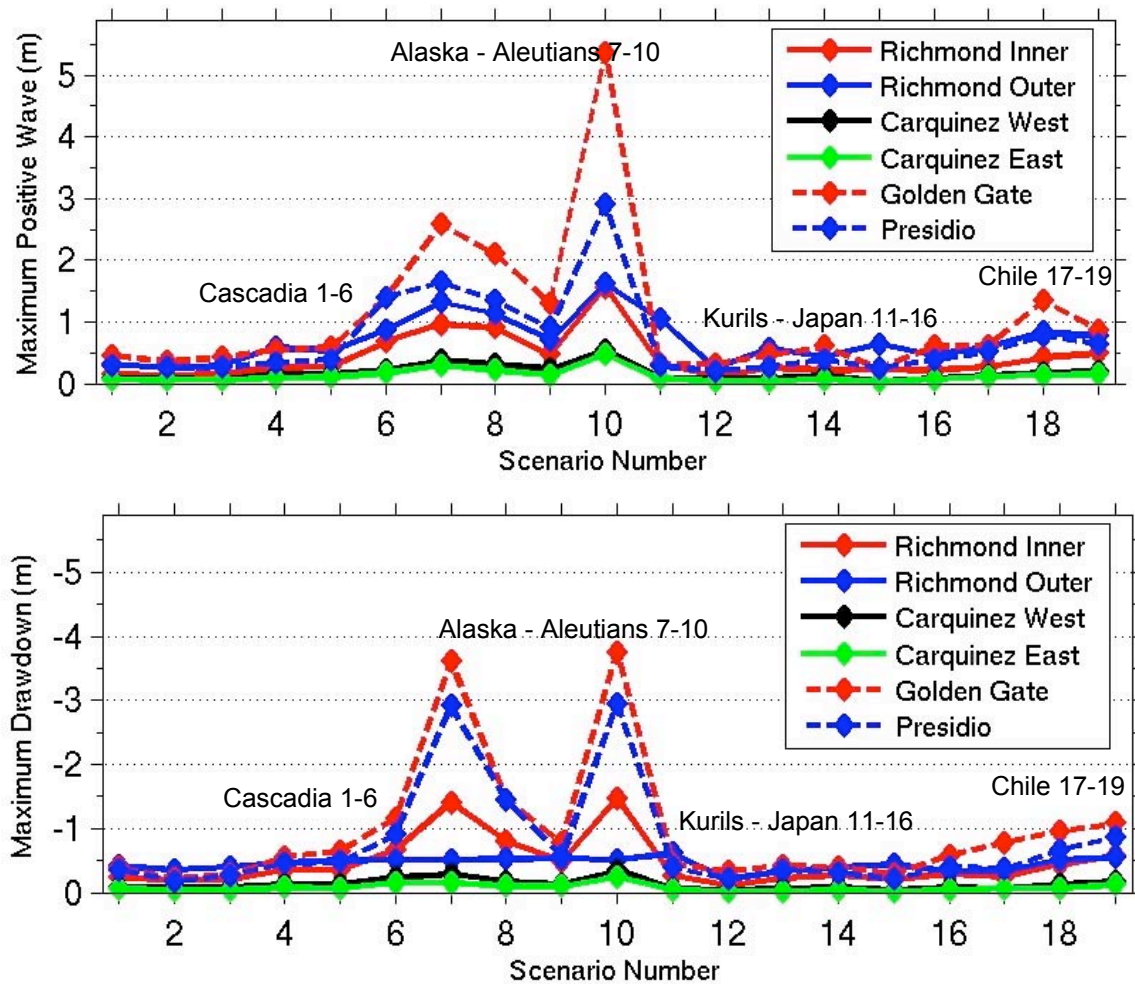


Figure 19 – Maximum positive (upper panel) and negative (lower panel) wave height for each scenario at specific locations within San Francisco Bay. The numbered source zones (1-19) – see tables 5 and 6 – are arranged from east to west with the South American sources listed last (numbers 17, 18 and 19, Table 7). Only sources from the Alaska-Aleutian Islands Subduction Zone produce positive or negative wave heights in excess of 1 m (3.3 ft) at an MOT location (i.e. Richmond Inner).

6.3 A WORST-CASE SCENARIO?

In an effort to create a plausible worst-case scenario, we combined historic information on past tsunamis affecting San Francisco Bay with our analysis of the tsunami response from displacements along the various subduction zone segments on the Pacific Rim. Since the largest response within San Francisco Bay results from displacements along the Alaska Peninsula segment of the Alaska-Aleutian subduction zone, we simulated the tsunami effects of a hypothetical $M_w = 9.2$ earthquake occurring along 800 km of this fault in the area of the zone most sensitive to San Francisco Bay response. This

earthquake would be similar in magnitude to the 1964 Alaskan earthquake or the 2004 Sumatra earthquake, however positioned along the Aleutian trench to give the largest impact in San Francisco Bay. For comparison, Figure 20 plots the simulated water levels for this event versus marigrams recorded during the 1964 tsunami.

The results suggest that the worst-case event would produce wave heights two to three times larger than what was experienced in 1964. Indeed the simulated wave heights and current speeds for this event are larger than for any other scenario that we modeled (See Appendices 1 and 2), however, they still do not reach the water heights estimated by Garcia and Houston (1975).

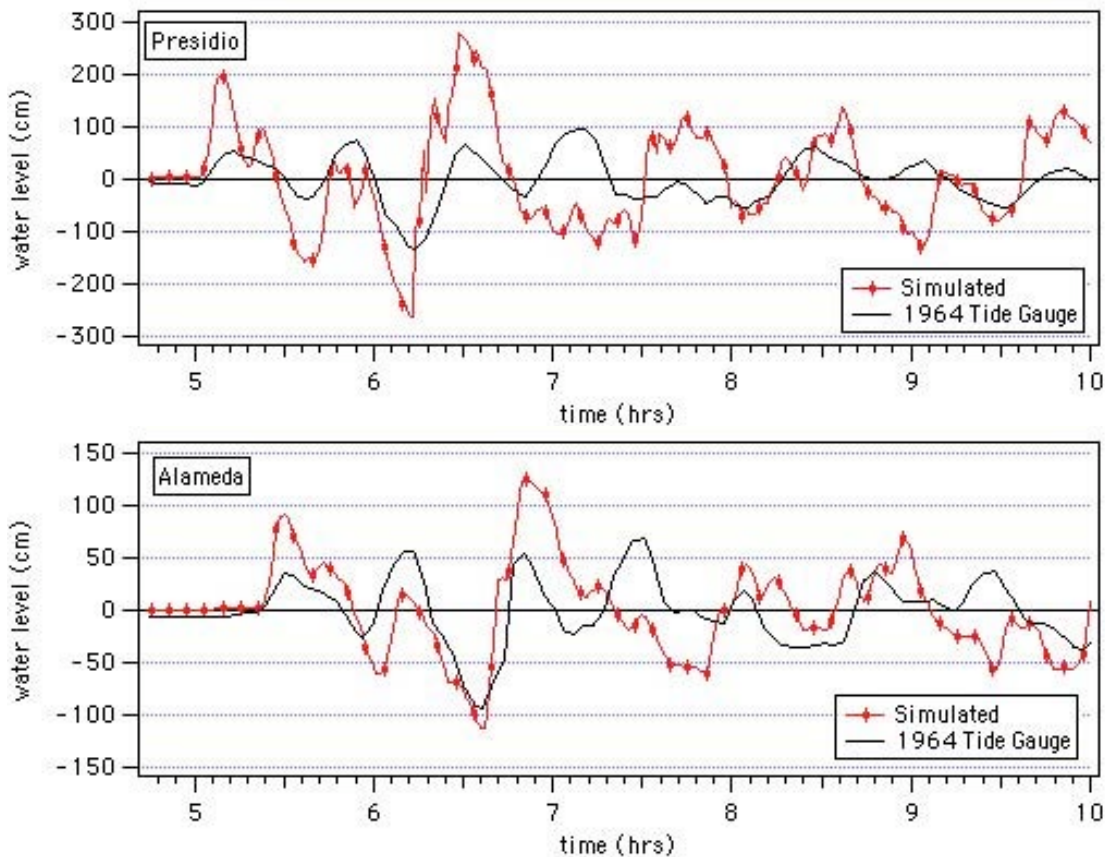


Figure 20 – Comparison between tide gauge records from the 1964 Alaskan tsunami and a simulated $M_w = 9.2$ earthquake generated tsunami at Presidio and Alameda.

Table 8 lists the maximum-modeled values for positive and negative water surface level at 6 regions inside San Francisco Bay for the largest far-field and local sources. The data suggest that the wave heights at the Carquinez Strait are on the order of 25% of the values seen at Richmond and 10% of those modeled for the Golden Gate. The terminals located in the Carquinez Strait show a much more muted response to the waves entering the Golden Gate. Table 8 also illustrates the attenuation from the Golden Gate to Richmond seen in Figure 15. For the outer Richmond area, the attenuation is on the order of 53% of the Presidio value whereas in the inner Richmond area, the attenuation is only 30%. These are both in the range of values for tsunami amplitude attenuation given by

Magoon (1966) based on his observations of the 1960 and 1964 tsunamis in San Francisco Bay and in line with the linear regressions shown in Figure 15, however the elevated wave heights for the inner Richmond locations should be noted. A more detailed study on the amplification of tsunami waves at the inner Richmond area should be performed to adequately explain the dynamics of this basin.

Region and Terminal ID	Far-field		Local	
	Wave height (+, m)	Wave height (-, m)	Wave height (+, m)	Wave height (-, m)
Richmond, outer (3)	1.56	-1.47	0.26	-0.18
Richmond, inner (1,5,6,11,12)	1.61	-1.62	0.44	-0.27
Carquinez, West (13,10)	0.55	-0.34	0.11	-0.21
Carquinez, East (7,9,14,15,16,17)	0.47	-0.24	0.10	-0.14
Golden Gate (19)	5.35	-3.74	0.60	-0.68
Presidio (20)	2.90	-2.93	0.40	-0.30

Table 8 - Maximum computed values of water surface rise and fall in meters for regions in San Francisco Bay from largest far-field and local tsunami sources. Numbers in parentheses correspond to locations in Figure 9. Note: 1 m = 3.28 ft.

Maximum-modeled current speeds for each site are listed in Table 9. The highest current speeds are seen in the inner Richmond area. These values are observed in the time record during rapid changes in the water surface elevation inside the semi enclosed basin where five oil terminals are located (see detailed time series plots in Appendix 1).

Region and Terminal ID	Far-field	Local
	Current speed (m/s)	Current speed (m/s)
Richmond, outer (3)	1.00	0.19
Richmond, inner (1,5,6,11,12)	2.73	0.62
Carquinez, West (13,10)	0.45	0.20
Carquinez, East (7,9,14,15,16,17)	0.42	0.16
Golden Gate (19)	2.88	0.51
Presidio (20)	4.98	0.47

Table 9 - Maximum computed values of current speed for regions in San Francisco Bay from far-field and local tsunami sources. Note: 1 m/s = 1.94 knots.

From the results of this study, it appears that the highest tsunami hazard exists for MOTs in the inner Richmond area from sources in Alaska and the Aleutian Islands. Inspection of animations of wave height plotted over time show how higher wave heights enter San Francisco Bay through the Golden Gate and propagate directly across the Bay into the Richmond, Berkeley and Oakland areas. All of the scenarios exhibit the long duration of wave activity that characterizes the marigrams from historic teletsunami events. The narrow waterway where these 5 MOTs are located is prone to resonant oscillations and this may be a cause of the elevated wave heights and current speeds seen here.

The study also suggests that near-field tsunami sources only present a second order tsunami hazard for marine facilities inside San Francisco Bay. The modeled wave heights and velocities for the largest near-field event (San Gregorio) are 25% or less of the largest far-field event (Aleutians III) (Tables 8, 9). We have included only one submarine landslide source in our scenarios, located in the Farallon Islands offshore of the mouth of the Bay. The bathymetry of San Francisco Bay is generally shallow with very gentle slopes and no history of massive slides into the Bay. Submarine landslides within the Bay are not considered a primary source for tsunami wave generation.

6.5 RECOMMENDATIONS FOR BAY AREA MOT SITES

We have conducted a deterministic study to identify the most severe events that could reasonably impact the Marine Oil Terminal sites in the San Francisco Bay area. The most significant historic event was the March 28, 1964 tsunami generated by the M_w 9.2 Alaska earthquake. In our modeled scenario runs, we simulated the 1964 event at the MOT sites. Of the 23-modeled scenarios, the event with the largest water heights and greatest water velocities within the Bay was a M_w 9.2 earthquake on the Alaska Peninsula segment of the Alaska-Aleutian subduction zone. This event generated peak water heights at the entrance to the Bay of over 5 meters. We note that our modeling results include uncertainties. Complex rupture in the source area and uncertainties in the bathymetry in the rupture area and along the tsunami travel path will cause some variation from the modeled results.

Table 10 – Water Heights and Current Velocities for Planning Purposes

ID*	Location	1964		Aleutians III	
		Height (m)	Velocity (m/sec)	Height (m)	Velocity (m/sec)
3	Outer Richmond	1.4	0.9	2.3	1.5
5	Inner Richmond	1.7	2.2	2.4	2.7
14	Martinez	0.3	0.4	0.7	0.2
10	Selby	0.5	0.4	0.8	0.5
13	Rodeo	0.5	0.3	0.8	0.6
17	Benicia	0.3	0.2	0.6	0.3
18	Portrero District, San Francisco	0.8	0.8	1.8	1.5
19	Entrance to San Francisco Bay	3.1	1.9	8.0	4.3
20	Presidio (Fort Point)	2.0	2.4	4.4	7.5

* See Figure 9 for location

For planning purposes we take a 150% factor of safety of our model runs for estimating peak water heights and current velocities for a 1964 event and for our worst-case scenario, the Alaska Peninsula rupture of the Alaska – Aleutians subduction zone. We consider this a conservative estimate; simulations of the 1960 and 1964 events suggest that our model slightly overestimates water heights and drawdowns. Table 10 summarizes our recommendations at the MOT locations. Note that the peak water levels can be in a positive or negative direction and peak current velocity direction varies and will be superimposed on the ambient tidal and flow regime in the Bay.

It is important to note that we assign no probabilities for any of the scenarios in our study. Recurrence estimates for Alaska 1964 events range from 350 years (Page et al., 1991) to 800 years (Plafker et al., 1992) and so this event does not likely represent the 50 to 100 year event as interpreted by Garcia and Houston (1975). There is no historic precedent for our “worst-case” scenario, a magnitude 9.2 event rupturing 800 kilometers from Kodiak Island to the Alaska Peninsula. The largest historic event on the Alaska Peninsula was a magnitude 8.3 earthquake in 1938 that produced a 0.2 m (.65 ft) wave at Crescent City but was not recorded within San Francisco Bay (Lander et al., 1993). Our Aleutians III scenario involves rupturing the western half of the 1964 rupture zone and continuing the rupture through the 1938 zone and into the Shumagin gap, an area of the Alaska-Aleutian subduction zone that has not produced an earthquake in historic times. There is no evidence to support or rule out such a rupture, but given the recent release of energy along the 1964 rupture, the likelihood of this event in the near future is very low.

Appendix 1 contains plots of the full time series for wave height and current speed for each terminal location for each scenario. Appendix 2 contains data tables for the maximum positive and negative water surface elevations and the maximum modeled current velocity and the direction of that flow. Appendices 3, 4, and 5 contain detailed historical information on the 1964 tsunami in San Francisco Bay and summarize recorded or observed events in San Francisco and in California. Appendix 6 contains data plots of the unprocessed tide gauge recordings from the 1960 and 1964 tsunamis at the Presidio and Alameda.

Acknowledgements

We thank the California State Lands Commission for funding this project. Martin Eskijian and John Freckman of the Commission initiated the project, spent hours meeting with us, discussed problems and progress and reviewed the manuscript. We particularly appreciate their patience over delays in the completion of this project caused by the 2004 Indian Ocean tsunami. Stuart Nishenko of PG&E and Orville Magoon of the Coastal Zone Foundation provided additional reviews. Geoffrey Legg gave programming assistance on bringing the FACTS Server on-line and Hemali Sutaria of USC helped to keep it alive. Jay Patton assisted in the compilation of GIS maps. Angie Venturato of NOAA/PMEL compiled the model bathymetry as part of the NTHMP TIME program.

References

- Aida, I., (1997). Simulations of large tsunamis occurring in the past off the coast of the Sanriku District, *Bulletin of the Earthquake Research Institute*, University of Tokyo, Vol. 52, 71-101.
- Bernard, E., Mader, C., Curtis, G., and Satake, K., (1994). *Tsunami Inundation Model Study of Eureka and Crescent City, California*, NOAA Technical Memorandum ERL PMEL-103, National Oceanic and Atmospheric Administration, Seattle, Washington, 80 pp.
- Bohannon, R. and Gardner, J., (2004). Submarine landslides of San Pedro Escarpment, *Marine Geology*, Vol. 203, 261-268.
- Borrero, J. C., (2002). Tsunami Hazards in Southern California. PhD thesis, University of Southern California, Los Angeles, California.
- Borrero, J.C., Gonzalez, F.I., Titov, V.V., Newman, J.C., Venturato, A.J., and Legg, G. (2004). Application of FACTS as a tool for modeling, archiving and sharing tsunami simulation results, *Eos Trans. AGU*, Vol. 85(47), Fall Meet Suppl., Abstract OS23D-1362.
- Barberopoulou, A., Qamar, A., Creager, K., Steele, W., Pratt, T., (2003). Local amplification of seismic waves from the M_w 7.9 Alaska earthquake and a damaging seiche in Lake Union, Seattle, Washington, *Seismological Research Letters*, Vol. 74(2), p. 245.
- Bruns, T.R., Cooper, A.K., Carlson, P.R., and McCulloch, D.S., (2002). *Structure of the Submerged San Andreas and San Gregorio Fault Zones in the Gulf of the Farallons off San Francisco, California, from High Resolution Seismic-Reflection Data*, in Parsons, T. ed., USGS Professional Paper #1658 Crustal Structure of the Coastal and Marine San Francisco Bay Region, California, 145 pp.
- Bromirski, P.D., Flick, R.E., and Cayan, D.R., (2002). Storminess variability along the California coast: 1858 – 2000. *Journal of Climate*, Vol. 16(6), 982-993.
- California Building Code, (2001). Title 24, Part 2, Chapter 31F "Marine Oil Terminals".
- Cox, D.C., and Morgan, J., (1977). *Local Tsunamis and Possible Local Tsunamis in Hawaii*, HIG-77-14, Hawaii Institute of Geophysics, November 1977, p. 118.
- Garcia, A.W., and Houston, J.R., (1975). *Type 16 Flood Insurance Study: Tsunami Predictions for Monterey and San Francisco Bays and Puget Sound*, Technical Report H-75-17, U.S. Army Engineering Station, Vicksburg MD, 267 pp.
- Geist, E.L. and Zoback, M.L., (1999). Analysis of the tsunami generated by the M_w 7.8 1906 San Francisco earthquake, *Geology*, Vol. 27(1), 15-18.
- Instituto Hidrografico de la Armada, (1982). *Maremotos en la costa de Chile*. Valparaiso, Chile, 48 pp.
- Jaffe, B.E., Borrero, J.C., Prasetya, G.S., Peters, R., McAdoo, B., Gelfenbaum, G., Morton, R., Ruggiero, P., Higman, B., Dengler, L., Hidayat, R., Kingsley, E., Kongko, W., Lukijanto, Moors, A., Titov, V., Yulianto, E., (in Press 2006). The December 26th 2004 Indian Ocean tsunami in Northwest Sumatra and offshore islands" in, Iwan, B., ed., *Earthquake Spectra*, Special Volume on the 2004 Indonesian Earthquake and Tsunami.

- Johnson, J.M., Satake K., Holdahl, S.R., and Sauber J., (1996). The Prince William Sound earthquake: joint inversion of tsunami geodetic data, *Journal of Geophysical Research*, V.101(B1), 523 – 532.
- Karl, H.A., Schwab, W.C. (2001), Landscape of the sea floor, in Karl, H.A., Chin, J.L., Ueber, E., Stauffer, P.H., Hendley II, J.W. eds, *Beyond the Golden Gate - Oceanography, Geology, Biology, and Environmental Issues in the Gulf of the Farallones*, USGS Circular 1187, 48-68.
- Lander, J.F., Lockridge, P.A., and Kozuch, M.J., (1993). *Tsunamis Affecting the West Coast of the United States 1806-1992*, NGDC Key to Geophysical Record Documentation No. 29, NOAA, NESDIS, NGDC, 242 pp.
- Magoon, O.T., (1962). The tsunami of May 1960 as it affected Northern California, *ASCE Hydraulics Division Conference*, Davis, California 18 pp.
- Magoon, O.T., (1966). Structural damage by tsunamis, *Proceedings, American Society Civil Engineers, Specialty Conference on Coastal Engineering*, Santa Barbara (California), Oct. 1965, 35-68.
- National Geophysical Data Center (NGDC) Historic Tsunami Data Base – online resource http://www.ngdc.noaa.gov/seg/hazard/tsu_db.shtml
- Okada, Y. (1985). Surface deformation due to shear and tensile faults in a half-space, *Bulletin Seismological Society of America*, Vol. 75, 1135-1154.
- Page, R.A., Biswas, N.N., Lahr, J.C., and Pulpan, Hans, (1991). Seismicity of continental Alaska, in, Slemmons, D.B., Engdahl, E.R., Zoback, M.D., and Blackwell, D.D., eds., *Neotectonics of North America*, in the collection The Decade of North American Geology Project series, The Geological Society of America, Boulder, CO, CSM V-1, 47-68.
- Parsons, T., Sliter, R. W., Geist, E. L., Jachens, R.C., Jaffe, B.E, Foxgrover, A., Hart, P. E., McCarthy, J., (2003). Structure and mechanics of the Hayward-Rodgers Creek Fault step-over, San Francisco Bay, California, *Bulletin Seismological Society of America*, Vol. 93(5), 2187-2200.
- Plafker, G., (1969). *Tectonics of the March 27, 1964 Alaska Earthquake*, USGS Professional Paper #543-I.
- Plafker, George, Lajoie, K.R., and Rubin, Meyer, (1992). Determining recurrence intervals of great subduction zone earthquakes in southern Alaska by radiocarbon dating: in Taylor, R.E., Long, Austin, and Kra, R.S., eds., *Radiocarbon After Four Decades: An Interdisciplinary Perspective*, New York, Springer-Verlag, 436-453..
- Raichlen F. and Synolakis, C.E., (2003). Waves and runup generated by a three dimensional sliding mass, in Locat, J., and Mienert, J. (eds.), *Submarine mass movements and their consequences*, Kluwer Academic Publishers, 113-119.
- Ritter, J.R., Dupre, W.R., (1972). *Map showing areas of potential inundation by tsunamis in the San Francisco Bay Region, CA*. Miscellaneous Field Studies Map MF-480, Environment and Resources Planning Study, USGS, Basic Data Contribution 52, 2 sheets.
- Satake, K., Wang, K., and Atwater, B. F., (2003). Fault slip and seismic moment of the 1700 Cascadia earthquake inferred from Japanese tsunami descriptions. *Journal of Geophysical Research*, Vol. 108(B11):E-7, 1–17.
- Soloviev, S.L., and Go, Ch. N., (1974). *A Catalogue of Tsunamis on the Western Shore of the Pacific Ocean*, Academy of Sciences of the USSR, “Nakua” Publishing House, Moscow, 1974, 310 pp. Translation by Canada Institute for Scientific and

- Technical Information, National Research Council, Ottawa, Ontario, Canada, 1984, 439 pp.
- Tanioka, Y., and Satake, K. (1996). Tsunami generation by horizontal displacement of ocean bottom, *Geophysical Research Letters*, Vol. 23, 861-864.
- Titov, V. V. and Gonzales, F. (1997). *Implementation and testing of the method of splitting tsunami (MOST) model*. Technical Memorandum ERL PMEL 112, NOAA, 11 pp.
- Titov, V. V. and Synolakis, C. E. (1998). Numerical modeling of tidal wave runup. *Journal of Waterway, Port, Coastal, And Ocean Engineering*, Vol. 124(4), 157-171.
- Topopozada, T.R., Bennett, J.H., Halstrom, C.L., Youngs, L.G., (1992). 1898 "Mare Island" earthquake at the southern end of the Rogers Creek fault, *Proceedings of the Second Conference on Earthquake Hazards in the Eastern San Francisco Bay Area*, California Dept. of Conservation, Division of Mines and Geology Special Publication 113, 385-392.
- USGS Fault Database – on line resource <http://earthquake.usgs.gov/qfaults/>
- Working Group on California Earthquake Probabilities (1999). *Earthquake Probabilities in the San Francisco Bay Region: 2000 to 2030 – A Summary of Findings*, USGS Open-File Report 99-517.
- Parsons, T. ed (2002). *Crustal Structure of the Coastal and Marine San Francisco Bay Region, California*, USGS Professional Paper #1658, 145 pp.
- Wentworth, C.M., Graham, S.E., Pike, R.J., Beukelman, G.S., Ramsey, D.W., Barron, A.D., (1997). *Summary Distribution of Slides and Earth Flows in the San Francisco Bay Region, California*, USGS Open-File Report 97-745C.
- Wiegel, R.L., (1955). Laboratory studies of gravity waves generated by the movement of a submarine body, *Trans. Am. Geophys. Union*, Vol. 36(5), 759-774.
- Wiegel, R.L., (1970). *Tsunamis in Earthquake Engineering*, Prentice Hall, Englewood Cliffs, N.J. 253-306.
- Wilson, B.W., Torum, A., (1967). *Final Report: Engineering Damage from the Tsunami of the Alaskan Earthquake of March 27, 1964*, Coastal Engineering Research Center, Corps of Engineers, U.S. Army, Contract No. DA-49-055-CIVENG-66-6, Science Engineering Associates, San Marino, CA.401 pp.
- Yeats, R.S., Sieh, K., Allen, C. R., (1997). *The Geology of Earthquakes*, Oxford University Press, New York, NY, 568.